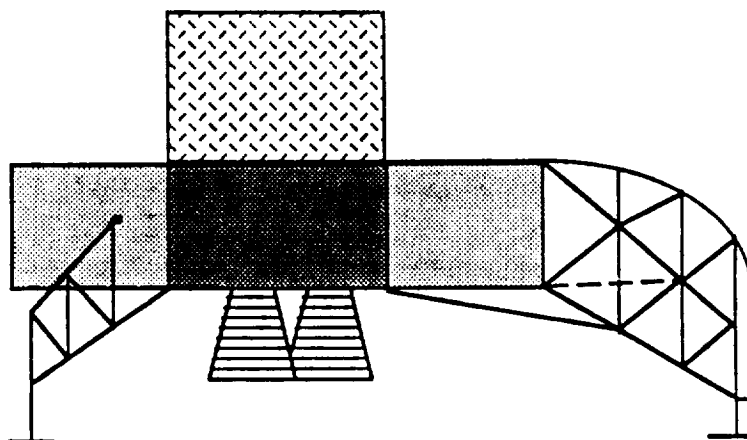


1 3 2
4444
p. 135

Final Design Report

for the

Self-Unloading, Reusable, Lunar Lander Project



Submitted to
Dr. George W. Botbyl
 The Department of Aerospace Engineering
 and Engineering Mechanics
 The University of Texas at Austin

B&T Engineering

December 7, 1990

(NASA-C9-189984) SELF-UNLOADING, REUSABLE,
 LUNAR LANDER PROJECT Final Design Report (B
 and T Engineering) 135 p CSDL 228

N92-24792

G3
 1/18

Unclass
 0073894

Final Design Report

for the

Self-Unloading Reusable Lunar
Lander Project

Submitted to
Dr. George W. Botbyl
The Department of Aerospace and
Engineering Mechanics
The University of Texas at Austin

B&T Engineering

December 7, 1990

B&T Employees

Ruwan Arseculeratne

Melissa Cavazos

John Euker

Fred Ghavidel

Todd J. Hinkel

John Hitzfelder

Jesse Leitner

James Nevik

Scott Paynter

Allen Zolondek

" Overall, we strive to give you the best service, dude"

Executive Summary

Introduction

In the early 21st century, NASA will return to the Moon and establish a permanent base. To achieve this goal safely and economically, B&T Engineering has designed an unmanned, reusable, self-unloading lunar lander. The lander is designed to deliver 15,000 kg payloads from an orbit transfer vehicle (OTV) in a low lunar polar orbit and an altitude of 200 km to any location on the lunar surface.

Mission/Trajectories

Initially the OTV transfers the lander from Low Earth Orbit (LEO) to Low Lunar Orbit (LLO). For maximum efficiency, the Earth-Moon transfer will be performed during the nodal alignment of LEO with the Moon's orbit. From a stable 200 km lunar polar parking orbit, the lander will wait for the orbit to align with the landing site longitude and then descend to the desired position on the Moon to deliver the payload. After the lander unloads the payload, it returns to the same polar orbit to await the arrival of another payload from an OTV. The total ΔV required for one mission is 3.594 km/s.

Payload System

The payload is carried on the top of the lander by a trolley system. The trolley system consists of a chain driven pallet which rides on two rails. The drive system consists of a continuous chain that is connected to the pallet's rear wheels and to a high torque drive motor. The drive system is sealed to protect from lunar dust contamination. The pallet and payload are supported in flight by detachable hardpoints. In order to unload the

payload, these hardpoints are detached and the pallet travels along the rails over the side of the lander, and down to the lunar surface. Then, the payload is detached from the trolley and the pallet is retracted. Although the payload is left on the surface, it is protected from the effects of the ascent engines by a distance of over nine meters and a minimum of blast shielding.

Docking and Refueling

Docking between the lander and the OTV is accomplished automatically. First, the lander soft docks with extendable columns on the OTV and then the columns are retracted, pulling the lander into a hard dock with the payload. Refueling is accomplished through fuel lines running through the support packaging of the payload. After refueling, the lander will detach with the payload from the OTV and begin the descent sequence of the mission

Lander Structure

The lander is made of four modular tank/subsystem boxes which surround the central engine/subsystem box that contains the main engines and avionics. These boxes have a rigid frame constructed of thin wall box beams and honeycomb sandwich panels. These panels provide torsional stiffness as well as thermal and dust protection. In addition to being supported by the structural boxes, the tanks have internal stiffeners/baffles. The lunar lander will touchdown on a four strut asymmetrical landing gear configuration. These struts will be equipped with a terrain adaptive system to help keep the lander level on uneven terrain.

Propulsion Subsystem

The main propulsion system consists of three H_2/O_2 engines capable of providing 30,000 lbs of thrust each. Only two engines are needed to lift the lander, and each engine has a 10° gimbaling capability for thrust correction in case of engine out and to adjust for center of mass location. In order to simplify the refueling process, the Reaction Control System (RCS) also uses hydrogen and oxygen. The RCS consists of vernier thrusters for low thrust maneuvers and primary thrusters for more substantial attitude changes. The RCS motors are placed at symmetrical positions around the lander on a horizontal plane.

Power Subsystem

The electrical power is supplied by a system of sodium-sulfide batteries for high power and mission operations, and gallium-arsenic solar photovoltaic arrays for recharging and on-orbit power during the time spent between missions. The photovoltaic arrays will be stored except when the lander is in LLO. These systems provide for peak power of 11 kW and nominal power of 0.5 kW. Peak power will be used for short durations in operations such as engine gimbaling and unloading. Nominal power is consumed by the lander systems that are in continuous operation.

Guidance, Navigation, and Control

The Guidance, Navigation, and Control (GN&C) subsystem will provide the lander with the ability to follow a pre-programmed mission objective. Guidance will be provided using two inertial measurement units (IMU) and two Dual Cone Scanners with Sun Fans to periodically update the IMU's. These systems provide all orbital parameters and attitude

information to the Navigation System. Navigation will consist of software in the central computer and a link with the communication subsystem to allow for input command signals to change or correct the mission. In addition, Global or Lunar Positioning System will provide position information as the Lander approaches the lunar surface. Rendezvous radar with transponders will be used for docking and refueling with the OTV as well as for the future case of landing near a lunar base. High precision imaging radar with obstacle avoidance software will provide the capability to land autonomously on the lunar surface. The Guidance and Navigation systems will send signals through the central digital computer to notify the Control System when maneuvers are required. The Control System will consist of RCS for relatively large attitude adjustments, a control moment system for fine tuning the attitude during proximity operations, and engine gimbaling for CM adjustments.

Communications

The three main communication links considered in this report are Lander-Earth, Lander-OTV, and Lander-Lunar Base. For Lander-Earth communications, a steerable S-band antenna will be used with infrared sensors for pointing. For Lander-OTV communications, X-band radar will be used for rendezvous and a low power VHF antenna will be used for transmission of data to be relayed to earth. The low power VHF antenna will also be used for communication with a lunar base. The communication with Earth will be performed through the Tracking Data Acquisition System (TDAS), the replacement for the present (Tracking Data Relay Satellite System) TDRSS system.

Thermal Control

The lander employs passive as well as active systems to maintain the temperature of the lander's subsystems. The lander's top side is designed to face away from the sun to radiate heat more efficiently. Radiators from active cooling systems are placed on this side, and the bottom side is insulated and covered with reflective coatings to protect the lander from the Sun's heat. While the cryogenic fuel of the lander is only protected by passive thermal systems, the boil-off of the fuel is still useable by the RCS thrusters.

Lander Mass Statement

The total deorbit mass of the lander is 49,376 kg which includes a 15,000 kg payload and 24,586 kg of propellant.

Table of Contents

Executive Summary	i
Appendices	x
List of Figures	xi
List of Tables	xii
1.0 Introduction	1
1.1 Requirements	1
1.2 Assumptions	2
1.3 Mission Scenarios	3
1.4 Top Down Design	4
2.0 Mission Narrative	6
3.0 General Description of Overall Design	8
4.0 Mission Description	10
4.1 Earth Departure	10
4.2 Lunar Operations	11
4.3 Descent/Ascent Trajectories	13
4.4 Sample Mission Scenario	15
5.0 Payload and Interface Systems	17
5.1 Docking Hardware	17
5.2 Docking Design Process	18
5.3 Docking and Refueling Procedure	19
5.3.1 Approach	19
5.3.2 Column Docking	19
5.3.3 Payload Docking	20
5.3.4 Refueling	21
5.3.5 Separation	22
5.4 Trolley System	23
5.4.1 The Unloading Process	23
5.4.2 Trolley System Hardware	24
5.4.2.1 Trolley Payload Pallet	24

5.4.2.2	Rail Channel	25
5.4.3	Lubrication	26
5.4.4	Dust Protection	27
5.5	Payload Protection	27
5.5.1	Blast Environment	27
5.5.2	Lunar Environment	28
6.0	Structures	29
6.1	Design Features	30
6.2	Main Structure	30
6.2.1	Engine Supports	31
6.2.2	Trolley/Lander Hard Points	31
6.2.3	Trolley Rail Support	31
6.2.4	Main Tank Integration	33
6.2.5	Docking Points	34
6.2.6	Subsystem Support	34
6.3	Landing Struts	35
6.4	Structure Materials	37
6.5	Lander Construction and Assembly	37
6.5.1	Modular Construction	38
6.5.2	Assembly and Refurbishing	38
7.0	Subsystems	39
7.1	Propulsion	39
7.1.1	Propulsion Requirements	39
7.1.2	Main Engine Design	40
7.1.2.1	Propellant Choice	40
7.1.2.2	Number of Engines	41
7.1.2.3	Engine Selection	41
7.2	Reaction Control System	42
7.2.1	RCS Configuration	42
7.2.2	RCS Propellant	43
7.2.3	RCS Propellant Feed System	44
7.3	Power Systems	46
7.3.1	Requirements	47
7.3.1.1	On Mission Time vs. Off Mission Time	47

7.3.1.2	High Power Mode	47
7.3.1.3	Low Power Mode	48
7.3.2	Power Subsystem Hardware and Operation	48
7.3.2.1	Active Mission Power Storage System	48
7.3.2.2	On-Orbit Power Supply Design	49
7.3.1	Power System Design	50
7.3.3.1	Active Mission Power Supply Design	51
7.3.3.2	On-Orbit, Constant Power Supply Design	52
7.4	Guidance, Navigation, and Control	53
7.4.1	Inertial Guidance	55
7.4.2	Navigation	56
7.4.3	Control	56
7.4.4	Data Processing and Management	57
7.5	Communication	58
7.5.1	Lander-Earth Communications	58
7.5.2	Lander-OTV Communications	59
7.5.3	Lander-Lunar Base Communications	59
7.6	Thermal Control System	60
8.0	Requirement Change	62
8.1	Light Fixed Unloader	62
8.2	Increased Payload	62
9.0	Reusability	63
10.0	Technology Development	64
10.1	Hydrogen-Oxygen RCS Fuel	64
10.2	Automated Docking and Refueling	64
10.3	Advanced Artificial Intelligence	65
10.4	Inertial Measurement Units	65
10.5	Tracking Data Acquisition System	65
10.6	Increased Cooling System Mission Life	66
11.0	Mass Statement	67

12.0 Management Structure	69
12.1 Managerial Communication	71
12.2 Program Schedule	72
13.0 Cost	74
13.1 Personnel Costs	74
13.2 Supply Costs	75
13.3 Computer Costs	75
13.4 Total Contract Costs	76
14.0 References	77

Appendices

Appendix A:	Design Process
Appendix B:	Descent/Ascent Trajectory Models
Appendix C:	Rocket Exhaust Plume Effects
Appendix D:	Vehicle Illustrations
Appendix E:	Propulsion
Appendix F:	Sample Calculations of Thrust
Appendix G:	Battery Sizing TK Solver Model

List Of Figures

Figure 1.1	The Top Down Design	5
Figure 4.1	Nodal Alignment of LEO's Orbital Plane with Moon's Orbital Plane	10
Figure 4.2	Accessible Longitudes	
Figure 4.3	Detail of Landing in a Flat Planet Approximation	14
Figure 4.4	Detail of Ascent in a Flat Planet Approximation	14
Figure 5.1	Lander Docking with OTV	17
Figure 5.2	Refueling Schematic	20
Figure 5.3	Trolley and Payload Locking System	21
Figure 5.4	Unloading Sequence	24
Figure 5.6	Rail Schematic	25
Figure 5.7	Rail Cross Section	26
Figure 6.1	Structural Design Features	30
Figure 6.2	Engine Supports	31
Figure 6.3	Trolley/Lander Hardpoints	32
Figure 6.4	Trolley Rail Support	33
Figure 6.5	Exploded View of Tank Support	33
Figure 6.6	Subsystem Support	35
Figure 6.7	Strut Configuration	36
Figure 6.8	Landing Struts	36
Figure 7.1	CG Range with 10° of gimbaling	42
Figure 7.2	RCS Thrusters	43
Figure 7.3	RCS Schematic	45
Figure 7.4	Vernier Thruster Schematic	46
Figure 7.5	Photovoltaic Array Schematic	50
Figure 7.6	GN&C Schematic	54
Figure 7.7	GN&C Block Diagram Description	54
Figure 7.8	Cooling System Schematic	60
Figure 12.1	Management Chart	70
Figure 12.2	Project Communication Schematic	72
Figure 12.3	Gantt Chart	73

List of Tables

Table 7.1	Hydrogen and Oxygen Performance Characteristics	40
Table 7.2	Engine Performance	41
Table 11.1	Mass Statement	67

1.0 Introduction

One of the future goals of space exploration includes returning to the Moon. This mission to the Moon will not be a short visit like Apollo, but will involve the establishment of a permanent lunar base to carry out long term scientific projects, such as selenology and astronomy. Creating a lunar base will involve the delivery of a significant number of payloads to the lunar surface. Therefore, an efficient and reliable delivery system is an essential element in the construction process of a lunar base. In order to meet this demand, B &T Engineering has designed an unmanned, self-unloading, reusable lunar lander.

1.1 Requirements

The design requirements for this lander come out of an AIAA Request For Proposal (RFP). The RFP requires comprehensive analyses and trade studies to be performed in order to select and size the vehicle and subsystems, develop the necessary scenarios, and define the operational procedures. The required design characteristics of the lander are:

- Capability to deorbit from Low Lunar Orbit (LLO) and land on the lunar surface with 7000 kg of payload plus the unloader plus fuel for ascent.
- Capability for the unloader to unload a payload equal to its own mass plus a 7000 kg package of the same diameter as a Space Station logistics module. This would allow the unloader to handle the payload from a lander which does not carry an unloader.
- Capability to be refueled and reloaded in LLO for another landing.
- Capability to carry the unloading mechanism back to LLO for later use at another landing site.

- Capability to return to LLO without the unloading device, to load a payload of mass equal to 7000 kg plus the mass of the unloader, and return to the landing site where the unloader waits.
- Capability to perform at least ten landing/unloading sequences before major servicing. A capability for additional sequences is desirable, but the abrasiveness of lunar dust may require frequent major servicing.
- Loader will not be required to provide cooling, power, etc. to the payload.

1.2 Assumptions

In order to design the lander, numerous assumptions were made concerning the requirements of the lander. The first set of assumptions deals with transporting the payload to the Moon. The overall payload delivery scheme will consist of three main transportation systems. One system will carry payload from the Earth's surface to Low Earth Orbit (LEO). The second system, an Orbit Transfer Vehicle (OTV), will transport the payload from LEO to LLO. Finally, the third transportation system, a lunar lander, will deliver payloads from LLO to the lunar surface.

The OTV is assumed to originally deliver the lander, or set of landers, to LLO. The current baseline assumption is that the OTV will carry a 15,000 kg payload package to LLO on each trip. In order to connect the payload package from the OTV to the lander, the payload packages are equipped with two sets of attach points. One set will be used to attach to the OTV, and the other set will be used to attach to the lander. This arrangement of connection points will decrease the amount of interface hardware between the OTV, payload, and lander. The lander will dock directly with

the payload and then the payload will detach from the OTV. Thus, the OTV will not need a manipulating arm in order to transfer the payload to the lander.

Once a payload package is transferred to the lander, the specific deorbit and landing sequence for that payload will be uplinked to the lander's control system. It is assumed that the general location for the placement of the payload on the lunar surface is determined by mission planners. Once the lander has deorbited and is over the general landing location, the onboard systems will determine the exact touchdown point for the lander. The lander will be able to detect the roughness of the terrain and determine whether the terrain is within the limits of the lander's landing system.

Another assumption is the definition of LLO. LLO is assumed to be a circular orbit with an altitude of 200 km. Due to lunar perturbations of the Moon, orbits less than 200 km can decay in as short a period as several months.

1.3 Mission Scenarios

After considering the AIAA requirements and the necessary assumptions, three main mission scenarios were developed. These missions include the supply of construction material for a lunar base, the delivery of payloads to remote sites, and the supply of an existing lunar base. The lander will be designed to accomplish all three missions.

The first mission is delivering equipment for the construction of a lunar base. Construction of the base will require a mobile crane device to assemble the equipment. This scenario can be broken into two cases, depending upon the availability of a mobile crane. In the first case, a fully

operational mobile crane will be delivered in the first landing. This crane would also be used to move cargo away from the landing site of the lander, greatly reducing the amount of blast protection required. Incorporating such mobility into the lander itself is inefficient, as is discussed in Appendix A of this report. In the second case, a crane may not operationally be available. Therefore, the payload must be landed in a landing pattern that provides a minimum safe distance between payloads. The payloads will be left in this pattern until an operational crane is available. Each payload will, then, be required to survive the blast effects of the lander. The second mission scenario is delivering scientific experiments to isolated locations on the lunar surface. Many experiment packages (such as astronomy and seismic experiments) will need to be located far away from the interference of other lunar facilities. This mission will require the delivery of payloads to various latitudes, possibly as high as the lunar poles. Blast protection for this mission is limited to one landing and ascent cycle.

The third mission scenario is resupplying an existing lunar base. This mission is the easiest mission to fulfill. With an established lunar base, landing facilities will exist which can move and protect payloads. In addition, these facilities will have prepared landing pads which will minimize the problem of blast deflection and navigation.

1.4 Top Down Design

The overall project goal of designing an unmanned self-unloading, reusable lunar lander has been broken down into five main tasks. These main tasks were broken down into smaller tasks. All of the tasks were determined by considering the project requirements, assumptions, and sce-

narios. The top down design (Figure 1.1) shows the breakdown of the project tasks that must be completed in order to accomplish the project's goal.

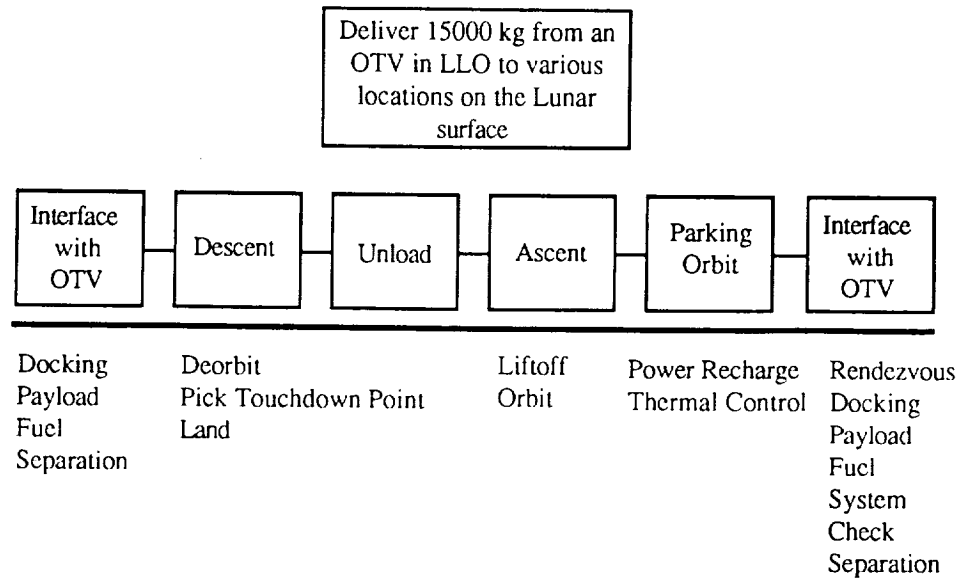


Figure 1.1 The Top Down Design

2.0 Mission Narrative

The transportation of cargo to the lunar surface will be accomplished in three phases. The first phase will boost the cargo into LEO. This phase will be accomplished with a lift vehicle such as the Space Shuttle. An OTV will then transport the payload from LEO to LLO. During the final phase, the reusable lunar lander will receive this cargo in LLO and deliver it to a predetermined site on the lunar surface.

The lander will be constructed on Earth and transported to LEO in modules. These modules will be assembled and inspected in space.

The assembled lander will be attached to an OTV, which will transport it to LLO with a lunar inclination of 90° and an altitude of 200 km. The lander will be delivered with sufficient fuel for station keeping. After inserting the lander into LLO, the OTV will return to LEO. Then another OTV will carry the first payload and the descent/ascent fuel to the lander's orbit. The lander will rendezvous with the second OTV and load the payload and fuel. The lander will then await its first deorbit point where it will begin its descent to the surface.

The lander will perform a system check and then a deorbit burn that will place it on an intercept trajectory with the surface. A second burn will be made approximately 250 meters above the surface to eliminate the remaining velocity. The lander will then perform a slow descent where it will use its high resolution radar to scan the immediate landing area so that a final landing site can be determined. The lander's terrain adaptive system will help keep the lander level as it touches down on an uneven surface. Once the lander has landed, another system check will be made. If the unloading system is operating properly it will begin to unload the cargo onto the surface.

The unloading process begins with a detachment of the trolley/lander hardpoints. The trolley motor will slowly move the trolley and the attached payload to the lunar surface. Once the payload is placed on the surface the trolley/payload attach points will disconnect and the unloaded trolley will be reeled back and locked into the trolley/lander hardpoints. Another system check will be made and the lander will begin the ascent burns.

The lander will use a two phase takeoff. This will consist of a low thrust initial burn followed by a high thrust burn. Takeoff is initiated with a low thrust burn so that the rocket plume effect on the payload will be minimized. These burns will place the lander on an intercept trajectory with the parking orbit. A final burn will be required to circularize the orbit. The lander will then wait in LLO for the next OTV.

To remain on station in the parking orbit, the lander will be required to perform some station keeping. Once in orbit, the lander will unfurl solar arrays so that the batteries can be recharged. The lander will also maintain a Sun-side facing attitude so that it can maintain suitable operating temperatures.

3.0 General Description of Overall Design

The self-unloading reusable lunar lander is a payload delivery system that transports up to ten 15,000 kg payloads from low lunar orbit to any location on the lunar surface within one service lifetime. The lander is made of four modular tank/subsystem boxes which surround the central engine/subsystem box. These modules are manufactured on Earth and are transported to LEO where they are assembled.

The lander is equipped with a self-unloading system. This system consists of a trolley which is attached to two rails which run from the top of the lander to the lunar surface. Payloads are attached to the trolley during the docking/refueling process with the OTV. Once the lander has reached the lunar surface, the trolley will move the payload from the locked position on top of the lander to the surface.

There are several subsystems that support lander operations. The lander is powered by chemical batteries and retractable solar photovoltaic cells. An inertial guidance system will be used for guidance. Navigation will be accomplished with mission software that may be updated from Earth. Control of the lander will be maintained by RCS motors, engine gimbaling, and control moment gyros. The on-board electronics will be actively cooled with a cold plate/radiator system. The spacecraft is equipped with a rendezvous radar and a high resolution radar for landing. Communication with Earth and the OTV will be maintained through S-Band and VHF radio transmitters respectively. Three main LO_2/LH_2 engines will provide the thrust for large ΔV 's. The LO_2 and LH_2 will be stored in four insulated tanks (two for each fuel type). The vehicle will land on a four

strut asymmetrical landing gear configuration. These struts will be equipped with a terrain adaptive system to keep the lander level on uneven terrain.

4.0 Mission Description

This section describes the OTV's departure from Earth, lunar orbital operations, ascent/descent trajectory models, and a sample mission scenario.

4.1 Earth Departure

The OTV transfers the lander from LEO to LLO. For mission planning purposes, the most efficient Earth-Moon transfer occurs every 9 days during nodal alignment of LEO with the Moon's orbit [1], shown in Figure 4.1. The Moon's orbital plane varies from 5.75° above the ecliptic plane to 4.85° below the ecliptic every 18.6 years. The Earth's equator is 23° above the ecliptic plane. Assuming that the OTV leaves LEO at a 28.5° inclination above the Earth's equator, the OTV will need to make an inclination change ranging from 33.65° to 44.25° . The ΔV required for these transfers ranges from 2.2 km/s to 7.3 km/s.[2]

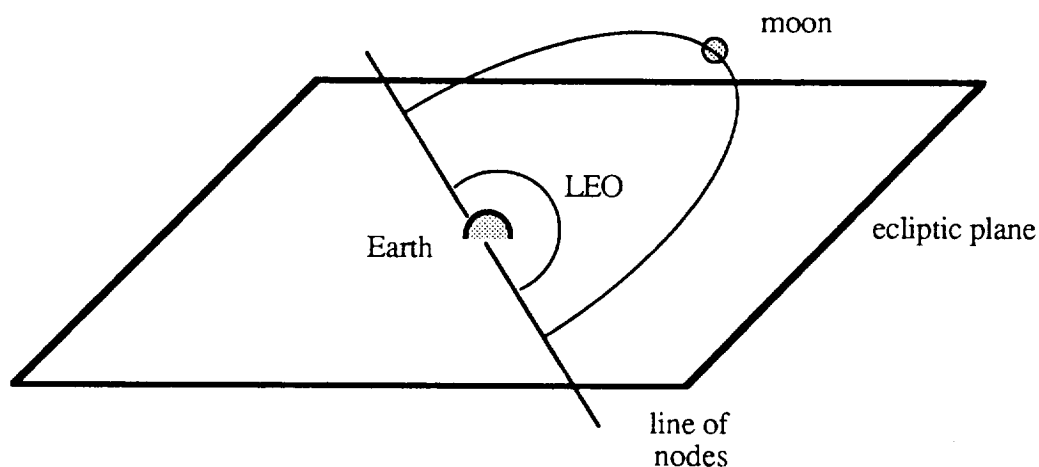


Figure 4.1 Nodal Alignment of LEO's Orbital Plane with Moon's Orbital Plane

If the plane change is made at the nodal crossing, the difference between reaching a lunar equatorial inclination and a lunar polar inclina-

tion is relatively small, the maximum being only 0.100 km/s [2]. An OTV is assumed to arrive approximately every two weeks to three months depending on the number of OTV's and their required turnaround times.

4.2 Lunar Operations

For lunar operations, a polar parking orbit with an altitude of 200 km will be used. A polar orbit was chosen because it provides accessibility to all latitudes and longitudes on the lunar surface. An equatorial or near-equatorial orbit would restrict the lander's access to higher latitudes. The longitude of the ascending node for a lunar polar orbit is not affected by perturbations. Therefore, the line of nodes will remain fixed relative to inertial space but will rotate relative to the Moon's surface, as shown in Figure 4.2.

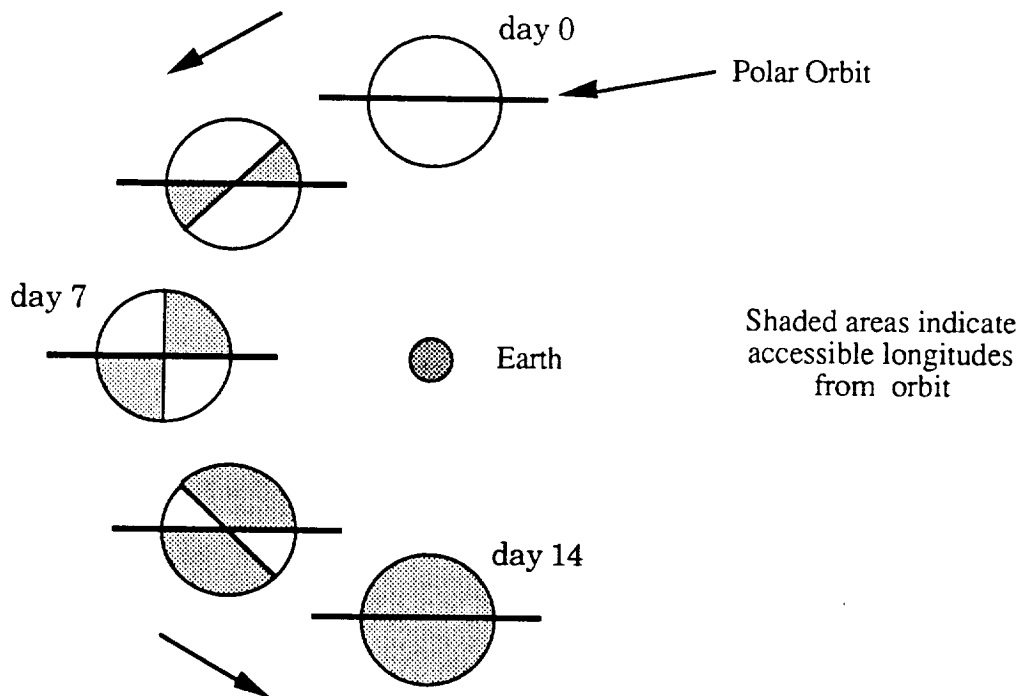


Figure 4.2 Accessible Longitudes

With the proper phasing, then, any longitude can be reached. The same site could be reached twice a month, when the line of nodes crosses the site's longitude and fourteen days later, when the site has rotated 180° with respect to the line of nodes.

After unloading the payload, the lander will ascend into the lunar polar orbit to wait for the next OTV. By waiting in orbit, the problem of propellant boil-off is greatly reduced. After ascent, a relatively small amount of fuel will be left in the lander. If the lander were left on the surface, extra fuel would be required for the ascent portion of the mission to compensate for the boil off. In orbit, this boil-off could be minimized by shielding the fuel tanks from the Sun. In addition, if a major malfunction were to occur with the lander, an OTV might still be able to rendezvous and recover the lander.

It was found that an altitude of 200 km provides a safe polar orbit. Due to lunar perturbations, the semi-major axis and eccentricity of a lunar polar orbit experience secular trends [3]. At lunar altitudes below 100 km, circular orbits decay to elliptical orbits and will impact the surface after approximately 300 days. At altitudes above 200 km, orbits cycle from circular to elliptical and back to circular again over a period of approximately every 750 days. Approximately once a year, the orbit reaches its lowest altitude of 120 km during periapsis passage. Although station keeping can keep the lander in a safe orbit at 100 km, the 200 km orbit was chosen because the lander can orbit indefinitely if it malfunctions or depletes its fuel.

A report on lunar polar orbits determined that an object orbiting at 100 km will need 0.3% of its total mass for station keeping fuel during a period of 1.5 months [3]. A 200 km orbit requires even less fuel for station keeping because the object's velocity is less than at a 100 km altitude. Using

the 0.3 % figure as an upper limit and the lander's total mass at the end of its ascent, this amounts to only 40 kg of fuel per month.

One disadvantage of a polar orbit is that a 'free return' is not possible in case of an OTV malfunction. Since the OTV is unmanned for our mission, the benefits of a polar orbit are considered to outweigh this drawback.

4.3 Descent /Ascent Trajectories

Descent and ascent trajectory models were developed in order to determine the amount of fuel required by the lander. These trajectories were modeled on TK Solver using the following assumptions: two-body problem, spherical Moon, instantaneous ΔV 's, and flat planet for the final and initial portions of the descent and ascent, respectively. These trajectory models do not include calculations of the ΔV 's required during hovering maneuvers, which take place just before landing. A factor of 1.1 was included in the amount of fuel determined in order to compensate for these maneuvers and the fuel lost to boil-off.

Descent and ascent trajectories were modeled as elliptical transfer orbits which intersect the Moon's surface. In the descent model (Figure 4.3), a deorbit burn in the 200 km parking orbit places the lander into its transfer ellipse. A second burn eliminates the intercept velocity at an altitude of approximately 250 meters. Finally, a third burn lands the vehicle on the surface. The ascent trajectory is modeled the same way as the descent trajectory, with the exception of a modified liftoff (Figure 4.4). The lander performs a low thrust takeoff to an altitude of approximately 100 meters, where a high thrust burn places the lander into the transfer ellipse. A low thrust takeoff minimizes the effect of the rocket exhaust on the payload. A

third burn circularizes the lander's orbit. The details of these models are presented in Appendix B.

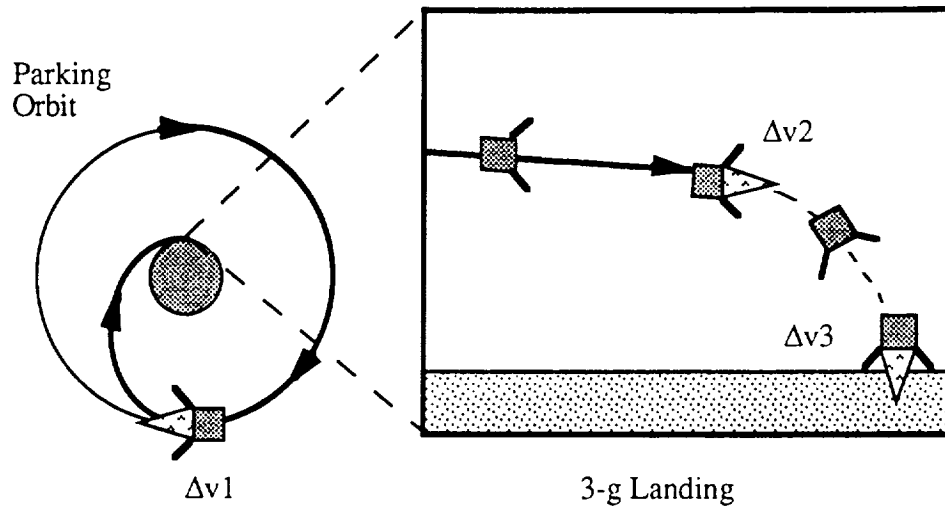


Figure 4.3 Detail of Landing in a Flat Planet Approximation

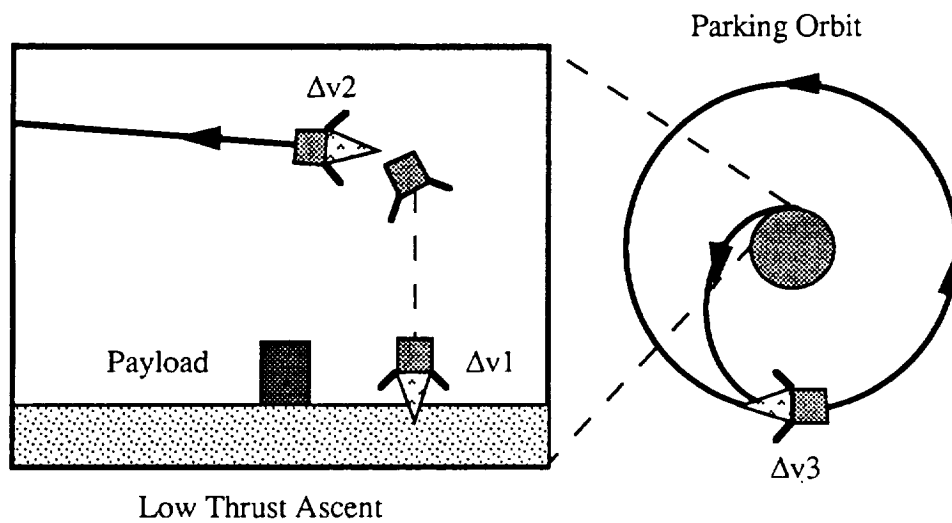


Figure 4.4 Detail of Ascent in a Flat Planet Approximation

4.4 Sample Mission Scenario

This sample mission gives the task sequences, ΔV 's, fuel requirements, and the mission time for the lander during a typical mission.

note: an OTV has already delivered the lander during a previous mission

Task	ΔV (km/s)	Fuel (kg)	Mission Time
<i>lander receives new payload</i>			<u>hrs:min:sec</u>
lander rendezvous and docks with the OTV	—	—	00:00:00
fuel is pumped into lander's tanks	—	—	01:00:00
system checkout	—	—	03:00:00
<i>lander descends to surface and unloads payload</i>			
lander separates from OTV (OTV returns to LEO)	—	—	03:05:00
first deorbit burn	0.046	550	03:20:00
<i>[radar continually scans surface during the descent]</i>			
second descent burn	1.715	16,789	04:19:40
final descent burn and landing	0.053	622	04:20:10
dust settles, system checkout, communication w/ Earth	—	—	04:25:10
unload payload, dust settles	—	—	04:30:10
system checkout, communication w/ Earth	—	—	04:35:10
<i>lander ascends to parking orbit</i>			
initial burn to clear payload	0.018	125	04:40:10
first ascent burn	1.718	5,647	04:40:21

final burn to circularize orbit	0.044	117	05:40:21
deployment of solar arrays, begin attitude control for thermal control	—	—	06:10:21

Summary

# Missions	# Restarts	ΔV (km/s)	Fuel (kg)	Mission Time
one	6	3.594	23,850	06:10:21

note: i) station keeping requires 40 kg/ month

ii) fuel masses include a factor of 1.1 to include fuel used during hover maneuvers and to compensate for boil-off

5.0 Payload and Interface Systems

This section discusses how the lander docks to the OTV to refuel and how payloads are loaded, transported, and unloaded.

5.1 Docking Hardware

The docking mechanisms ensure that the lander and the OTV will be properly and safely attached and that the payload and refueling connections are aligned. This section describes the hardware, and the next section describes the docking procedure.

The docking hardware for the OTV and the lander is shown in Figure 5.1. The lander is equipped with female connectors on the top side and the OTV has male connectors on two extendable docking columns, one primary and one secondary. The functions of the docking columns are to align the vehicles and control the connection of the lander to the payload.

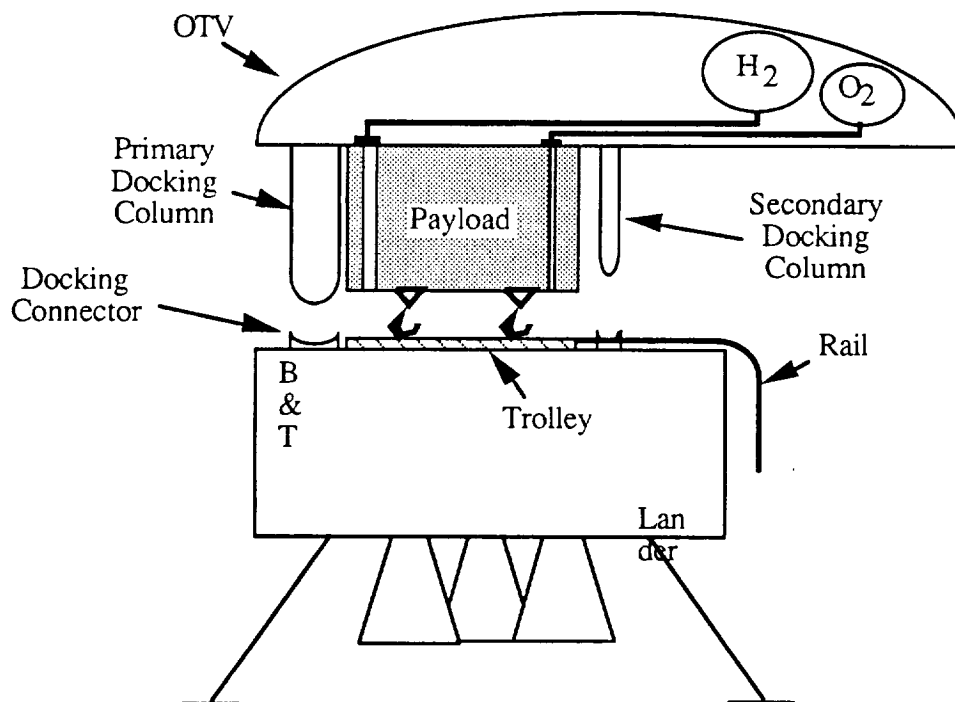


Figure 5.1 Lander Docking with OTV

The primary column is extended further out than the secondary and both extend past the payload on the OTV, as shown in Figure 5.1. The lander first contacts the primary column which is designed to take loads from the relative velocity of the vehicles and aligns them correctly for hard docking.

Refueling is accomplished through fuel lines which are attached to the payload. These refueling lines are attached to the payload instead of the docking columns because the columns have to be extendable. Another option that was researched was the use of flex lines. These lines were not used because they are prone to leaking and have a limited range of movement [4].

5.2 Docking Design Process

Docking was designed to be an automatic procedure, capable of transferring the payload and fuel safely without a complex robotic manipulator system. The docking mechanisms were integrated with the payload, because docking occurs along the line of center of mass for each vehicle, and the payload must also be carried on the line of center of mass [5]. Since the weight of non-reusable payload fittings was also a concern, the soft docking mechanisms were not placed on the payload. This moved the initial docking away from the line of the center of mass of each vehicle, causing a problem with maintaining the attitude of the vehicles during docking. However, the automatic docking system, guidance, navigation, and control can solve this problem.

Directly docking with the payload and requiring the OTV to have a manipulator system were also considered. Docking directly to the payload was not acceptable, since the payload would have to support all docking loads and the docking mechanism on the payload would be left on the lunar

surface. An OTV manipulator system was rejected because remote operations are difficult and extendable refueling lines are required.

5.3 Docking and Refueling Procedure

This section will describe in detail the sequence of events for docking and the function of each mechanism.

5.3.1 Approach

Docking will begin with the insertion of the OTV into the lander's parking orbit (Section 4.2). During the approach phase, the OTV and lander will use their rendezvous radars to attain proper alignment (Section 7.5.2), much like the automatic docking procedure used by the Soviets [6]. The control moment gyros (CMG) and the gaseous H_2/O_2 vernier thrusters will be used to control the trajectory of the lander. Once the OTV and the lander are sufficiently close (within 100 meters), the vehicles will perform RCS burns to slow their relative velocity to less than one m/s. The docking mechanisms of the vehicles will be readied and checked by onboard computers to ensure that they function before actual docking is attempted. Next, the OTV will make final corrections to the lander's position and attitude during approach and will maneuver so that the mechanisms contact for soft docking.

5.3.2 Column Docking

Soft docking occurs when the male connector of the primary docking column on the OTV contacts the primary female connector of the lander. The soft docking aligns the two vehicles and latches the primary column on the OTV into a hard dock when the vehicles are correctly aligned.

Next, the secondary docking column on the OTV is extended to the lander to connect to the lander's secondary female connection. The secondary column is necessary to ensure that the relative attitude of the vehicles is correct so that the payload fittings and refueling lines will properly connect to the lander (Figure 5.2). The two docking columns will retract at the same rate until the lander contacts the payload. Since the retraction is completely controlled by the OTV, the throw-away structure on the payload is minimized.

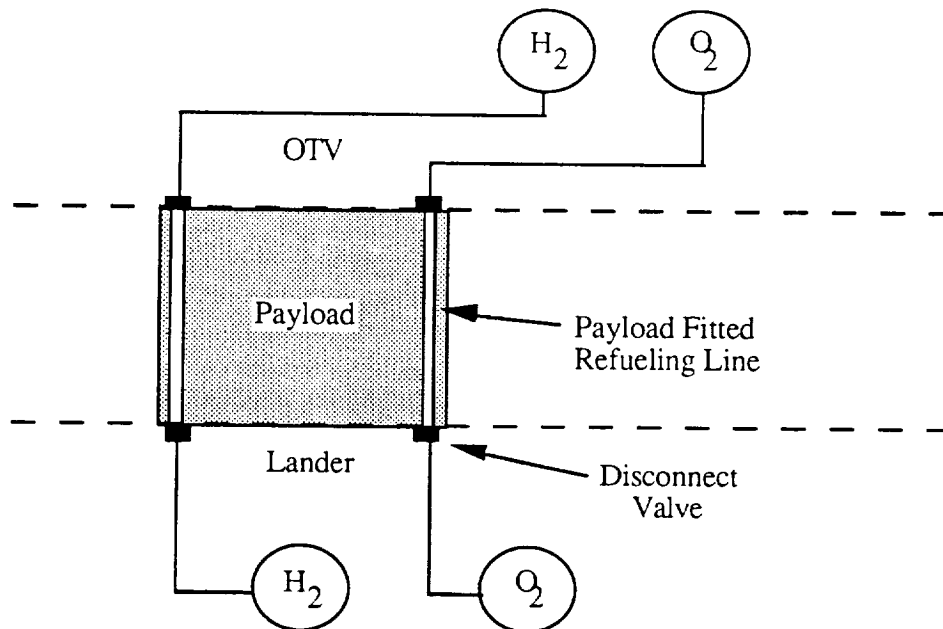


Figure 5.2 Refueling Schematic

5.3.3 Payload Docking

The lander will connect to the payload through a pallet (the trolley). As shown in the Figure 5.1, the payload will be aligned to contact the trolley when the docking columns retract. Connection between the trolley and the payload will be through mechanisms similar to car door latches, with the clamping device on the lander, as shown in Figure 5.3 [7]. The mechanism

locks on impact and is opened electro-mechanically. The trolley will have four of these connections, centered about the center of mass (CM) of the lander.

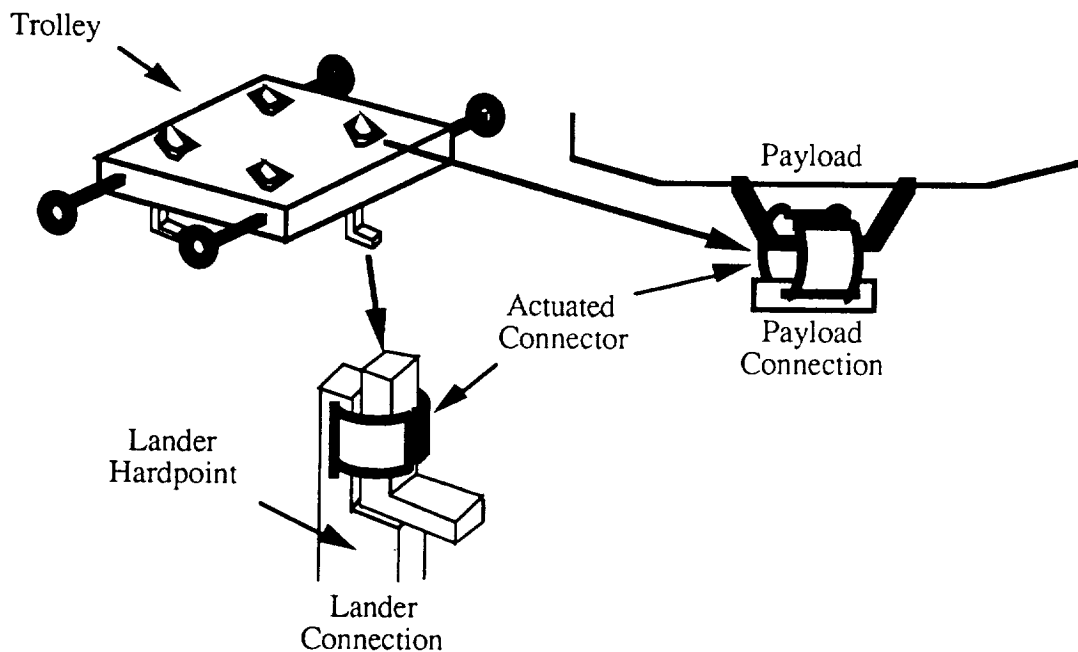


Figure 5.3 Trolley and Payload Locking System

5.3.4 Refueling

Refueling uses fuel lines which are attached to the payload. The valves for the lines are in the OTV and the lander, so the lines in the payload will be merely straight piping. The piping extends above and below the payload into the OTV and lander. The fuel lines of the OTV and the lander have an extendable end portion that is electro-mechanically actuated to meet the piping from the payload. This action depresses the dust boot that covers the fuel lines. A collar is then extended over the two lines to seal the connection. This process is shown in Figure 5.4. After the connections

have been sealed on both the OTV and the lander, valves are opened and the fuel is transferred to the lander. A similar system is used during Mir space station operations [5].

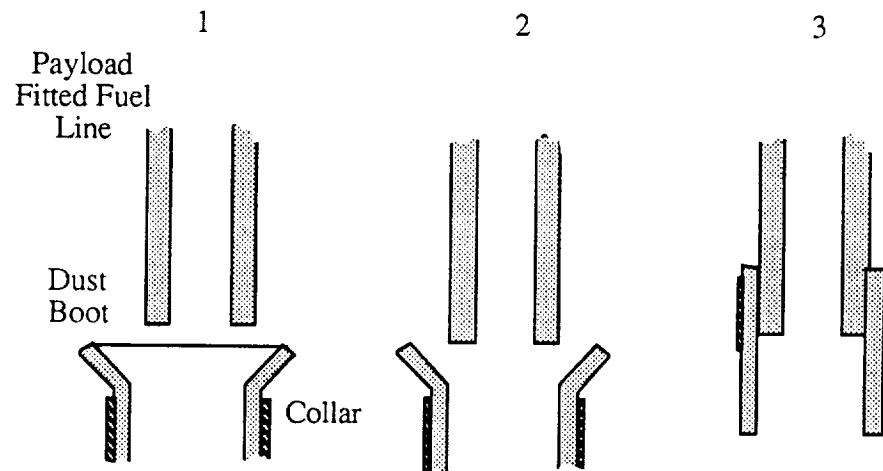


Figure 5.4 Fuel Coupling Sequence

The OTV is required to provide the pressure to transfer the fuel to the lander. A possible solution would be to pump Helium, kept in a separate tank, into the H_2 and O_2 tanks to force the fuel out. A pump would be used to avoid providing the mass for a high pressure tank and Helium would be used to prevent the problems incurred when pumping cryogenic hydrogen and oxygen.

5.3.5 Separation

Separation will begin with the valves of the refueling lines closing. Since the payload must be protected from any docking loads, the connections between the payload and the OTV must be disconnected first. Next, the latches on the docking columns will disconnect and the docking

columns will be retracted. Still controlled by the OTV, the lander will use its vernier RCS to separate. After a safe separation distance has been achieved, the lander can independently proceed with the rest of the mission.

5.4 Trolley System

The unloading system consists of the trolley, connected to wheels inside a closed rail. The payload is connected to the trolley and is lowered to the lunar surface as it travels along the rail. This section describes the unloading process and the trolley system.

5.4.1 The Unloading Process

The trolley begins in a locked position, supported by connections to lander hardpoints. The connections are similar to those used to connect the payload to the trolley, as discussed in Section 4.3.3. The trolley stays in this locked position for all orbital maneuvers and landing.

Once safely landed, the trolley will unload the payload. As shown in Figure 5.5, the payload travels along the rail and down the side of the lander to the lunar surface. This figure shows that the payload is raised above the rail so that binding is prevented. Once resting on the lunar surface, the payload is released from the trolley attachments and the trolley is returned to its locked position.

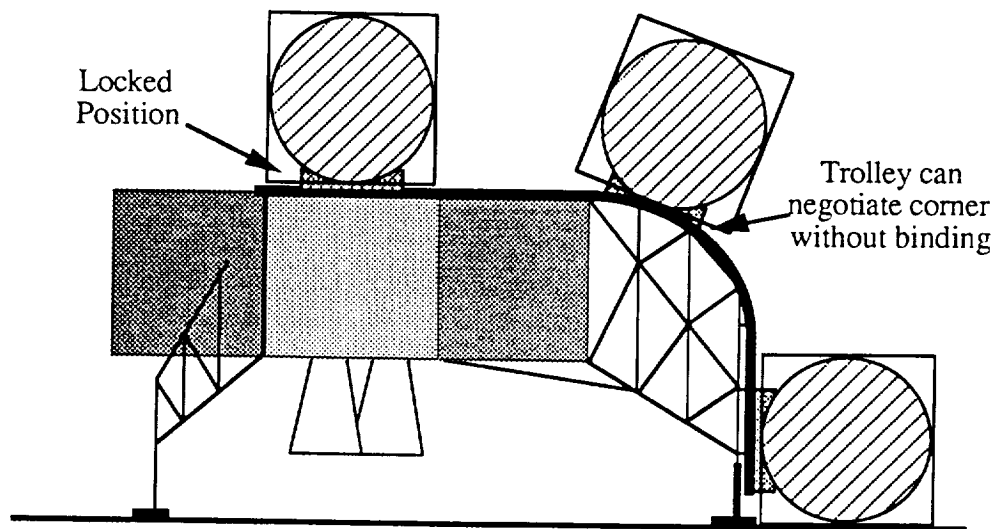


Figure 5.5 Unloading Sequence

5.4.2 Trolley System Hardware

This section describes in detail the individual trolley system components and their functions.

5.4.2.1 Trolley Payload Pallet

The trolley, shown in Figure 5.3, is an aluminum honeycomb box with two axles and four wheels. The wheels fit into the channel of the rail and the axles support the trolley when the payload is being unloaded.

The trolley connects the payload to the lander through the use of electro-mechanical clamps that operate similar to the mechanisms of a car door [7]. The clamps are closed by impact and are opened electro-mechanically. Operation is powered by a small, replaceable battery contained within the trolley that will last for at least ten missions. Operation is controlled by a radio link to the computers of the lander.

When the trolley is in the locked position, the four clamps are centered about the center of mass of the lander. To connect to the lander in this

locked position, the trolley has attach points on its underside. These attach points form the receptacle for clamps that are connected to hardpoints on the lander. As can be seen from the arrangement in Figure 5.3, the hardpoints will support the trolley and payload so that the axles of the trolley do not support them during the accelerations from engine firing and landing.

5.4.2.2 Rail Channel

The rail, shown in Figures 5.5 and 5.6, begins at the trolley's locked position and travels along the engine box (section 6.2.3), over a Hydrogen tank, and down the unloading side landing truss. The chain is completely inside the rail channel and returns to the motor through a secondary return channel. The rail is connected directly to the lander. The rail shape is maintained by a simple truss structure integrated into the landing struts.

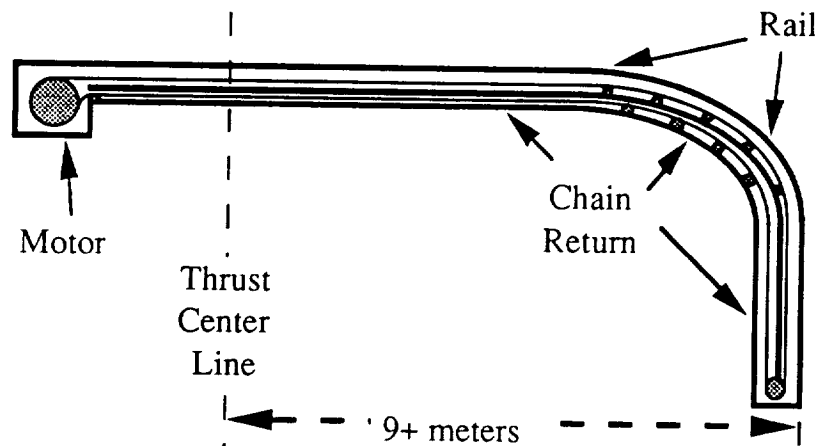


Figure 5.6 Rail Schematic

The cross section of the rail channel is presented in Figure 5.7. The rail is enclosed to prevent the wheels from going off track and to shield the mechanism from lunar dust. Further lunar dust protection is provided by the dust baffle, which is an extension of the rail channel around the axle.

Lunar dust protection is discussed in Section 5.4.4. A dual wheel was used so that the chain would pull only in the direction of motion and not bind the mechanism. This minimizes the wheel sticking if the channel is blocked by lunar dust or if the wheel cannot roll. Guides are also provided for the chain to aid in negotiating the turns of the channel. Guides are also provided for the chain to aid in negotiating the turns of the channel.

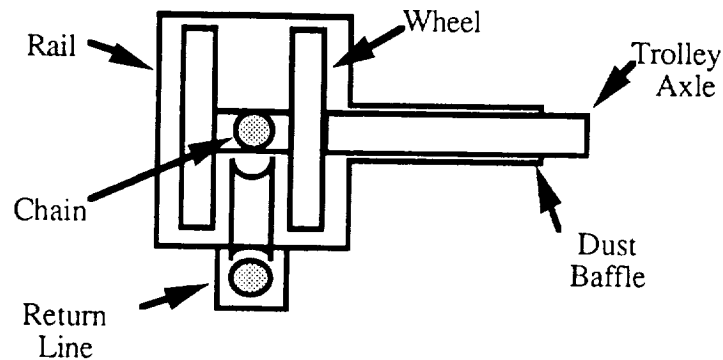


Figure 5.7 Rail Cross Section

5.4.3 Lubrication

Lubrication in space is a very difficult problem. However, common lubricants on Earth do not work well in space. Lubricants sublime under the low pressure and either boil off or freeze due to the temperature extremes. Solar radiation can also degrade lubricants.

A possible candidate has been found to lubricate the bearings of the trolley wheels and the other moving parts of the lander. Molybdenumdisulfide, MoS_2 , is a solid lubricant applied by a radio frequency sputtering operation. It has been tested in a vacuum and was determined to have excellent endurance and performance for rolling friction [8]. A full technical analysis of this problem must be performed and solved.

5.4.4 Dust Protection

Lunar dust is known to cause harmful effects on mechanisms. For the lander's mechanisms to survive ten missions, they must be protected from the lunar dust. The primary mechanism open to intrusion by the regolith is the trolley and rail. As shown in Figure 5.7, the opening is restricted by a dust baffle. This should greatly reduce the amount of dust entering the rail.

Another quality of the lunar dust is its electrical conductivity, which is very low. Furthermore, as a consequence of exposure to visible and ultra-violet radiation from the Sun, the conductivity of the lunar soil changes with temperature. This effect is great enough in the contrast between lunar day and night that a lunar "dust storm" of particles could follow the solar terminator, levitated by electrostatic charges between the particles. During lunar night, disturbances of the lunar soil could raise dust clouds that would coat exposed surfaces of a mechanism [9]. This effect would be extremely hazardous to lander operations. A possible solution to this problem is to install an electromagnet along the rail channel openings with the current set so that the magnetic field will repel the charged dust.

5.5 Payload Protection

An extensive study was done to investigate the rocket exhaust plume effects (Appendix C). From this study, it was concluded that payload protection would be necessary.

5.5.1 Blast Environment

To prevent damage to the payload from the lander's rocket plume during ascent, a system must be developed which can withstand the high

temperatures and high velocity particles contained in the rocket exhaust plume. A system similar to the protective blanket suggested in reference [10] could be used, provided it can withstand the high temperatures of the exhaust plume. The blanket would be a self-deploying system composed of multiple layers of impact and thermal protection. Another concept that should be investigated as blast shielding is simply turning the hot, high velocity particles away from the payload with some type of deflector. Also, the idea of attaching an ablative material to the payload should be investigated. Whichever method is chosen, it should be light-weight, compact and easily deployable. Also, the protective system material must not deteriorate in the vacuum of space.

5.5.2 Lunar Environment

Since a protective system will already be in place for rocket exhaust effects, adding additional systems to protect the payload from radiation heating of the lunar environment and micrometeorite impacts may not be necessary. Even if further protection is required, the blanket system conceptualized in reference [10] could be attached to the payload, providing additional protection. The blanket would be self deploying and composed of multiple layers of impact protection and thermal protection. As suggested in reference [10], a blanket could later be used as a "regolith support cloth or surface garage". This system would protect the payload from large temperature variations and high velocity particle impacts, while only weighing about 1.3% of the total payload.

6.0 Structures

Due to the hardware intensive nature of this project, the design of the lander structure was considered in some detail. These considerations remained conceptual in nature, since detailed structural analysis was beyond the scope of this project.

The structure provides connectivity and integrity to all systems. During the structural design process, the types and magnitudes of loads must be known and accounted for. The typical loads encountered by the lander include:

- Engine firing loads
- Impulsive landing loads
- Static loads after touchdown
- Quasi-static loads during unloading
- Inertial loads of all components during acceleration and deceleration

The basic philosophy in the design of the lander was to consolidate as many of the forces that would be encountered into the same components to increase the overall efficiency of the structure. A complete set of views of the lander is given in Appendix D.

6.1 Design Features

In developing the basic structural concepts, the precedents set by the Apollo program were used. The lower stage of the Apollo lander was a monocoque type construction that consisted of four structural boxes joined together to form a central box. The four boxes housed the fuel tanks and were the attach points for the landing gear. The central section housed the descent engine [11]. A similar approach was used in the basic design of the

reusable lunar lander. This design combines the forces into the central box region.

Due to the demanding nature of the lander's proposed mission, which includes a 15000 kg payload and the ability to perform 10 missions without repair, a stronger structure than the Apollo lander is necessary. Increasing the overall strength and stiffness will be accomplished by using thin wall box beams to form the perimeter of the boxes and honeycomb core panels for the sides of the boxes (Figure 6.1).

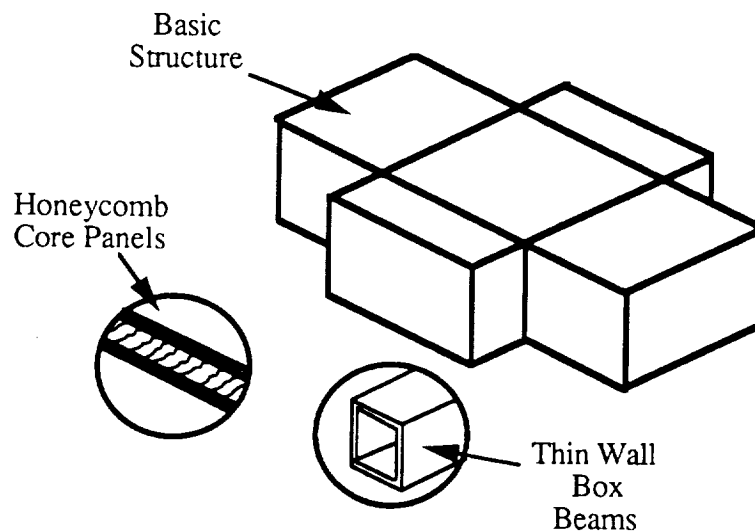


Figure 6.1 Structural Design Features

6.2 Main Structure

The components that must be supported by the main structure include the engines, fuel, Payload/Trolley system, docking points and sub-systems.

6.2.1 Engine Supports

The lander will use a three engine arrangement (Section 7.1.2.2) connected to a common triangular subframe. The subframe will be very rigid, providing the base on which the engines will pivot for gimbaling. The engine subframe will in turn be connected to the central box via a series of members (Figure 6.2). These axial members are constructed so that the catastrophic failure of any one member will not be fatal to the engine support structure.

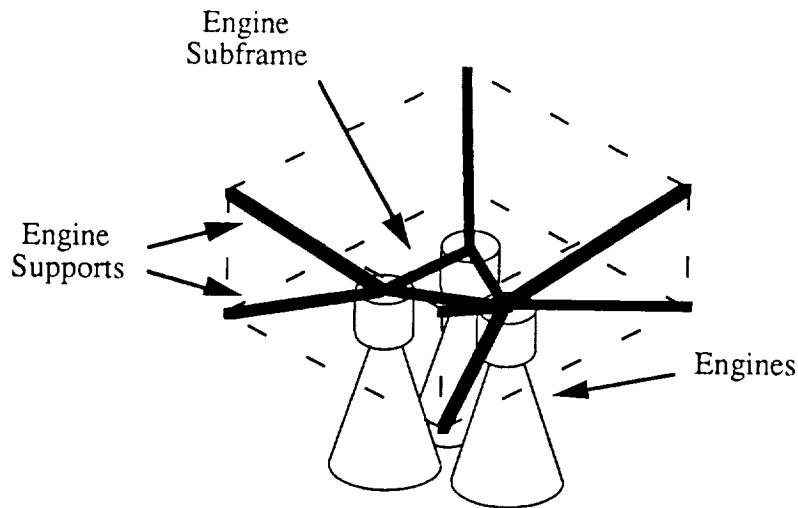


Figure 6.2 Engine Supports

6.2.2 Trolley/Lander Hardpoints

The detachable hardpoints which join the trolley and payload to the lander will be connected directly to the engine subframe. This connection will be done through three pylons which will run from the subframe through the main subsystems bay so that it can interface with the trolley (Figure 6.3). This allows the direct transmission of engine thrust forces to the payload and the utilization of the engine supports for the support of the payload after touchdown. The failure of one of these pylons will require that

the trolley support axles carry the unsupported loads. Under normal flight and landing conditions, these axles should be sufficient to properly support the payload without over-stressing the trolley mechanism.

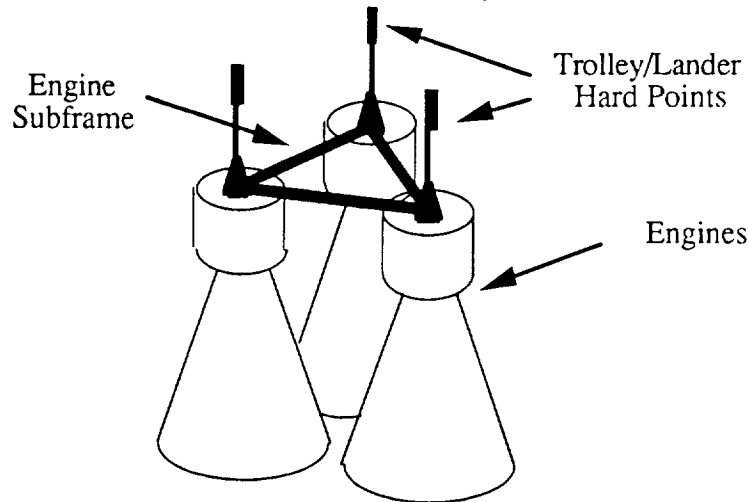


Figure 6.3 Trolley/Lander Hardpoints

6.2.3 Trolley Rail Support

The rail of the unloading system will be supported by the walls of the central box and the tank box of the forward H_2 tank while it is on the main body of the lander (Figure 6.4). The forward landing struts will provide the support for the payload as it is moved off the lander and to the lunar surface (Section 5.4.1). The landing struts incorporate a terrain adaptive system that will prevent the trolley rail from binding. The tank box for the forward H_2 tank will need some extra stiffening to support the payload as it is being unloaded. Since the main body of the lander is the support for the rail, only a major structural failure can disable the it.

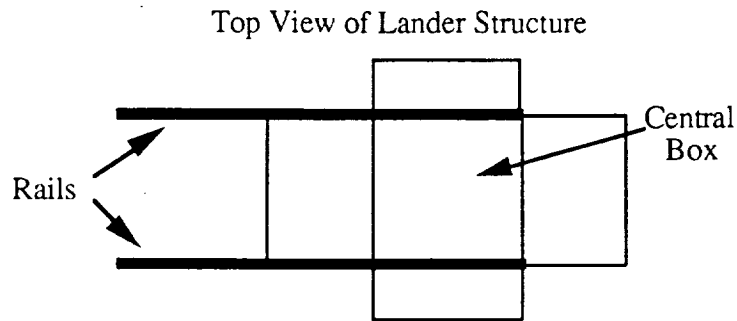


Figure 6.4 Trolley Rail Support

6.2.4 Main Tank Integration

Integration of the main fuel tanks into the main structure is crucial in the design of the lander, since the fuel makes up almost half of the total weight when the lander is fully fueled. The tanks were chosen to be cylinders with hemispherical endcaps since they are easier to support in a cantilever fashion. The tanks will be supported in the tank boxes as shown in Figure 6.5. In addition to these supports, the tanks will have internal support to increase their stiffness. The supports will be shaped so that they act as baffles to prevent fuel sloshing while the lander is in flight. A breach in the tank wall could be fatal to the mission. Such a failure would occur only if adverse forces were applied to the lander.

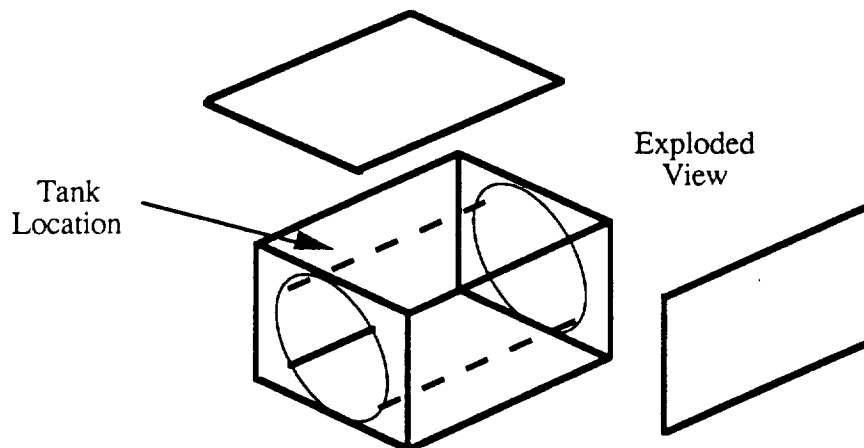


Figure 6.5 Exploded View of Tank Support

6.2.5 Docking Points

The lander will have two main docking points. The primary dock will make initial contact during the mooring phase of the docking procedure and the secondary dock will be used to help maintain precise control between the lander and the OTV (Section 5.1). Since docking will occur at zero g and close to zero relative velocities, the docks will not be required to support large forces. The docks themselves will be placed on the top skins of the H₂ tank box and will be supported by a light subframe that will connect them with the central box to prevent the H₂ tank box from taking the load.

6.2.6 Subsystem Support

The subsystems of the lander include the power system, GN&C, communication, thermal control, and the central computers. These systems are not significantly massive, but some of these systems require stable platforms. The current subsystem configuration places most computer systems in the main subsystems bay (Figure 6.6). Also included in this bay are the control moment gyros that are used for attitude control. The secondary bays (A & B) house the power system (excluding solar arrays), RCS, radios, and the thermal control system. Each bay will be thermally insulated from its surroundings with removable panels and will be sealed to prevent contamination by lunar dust.

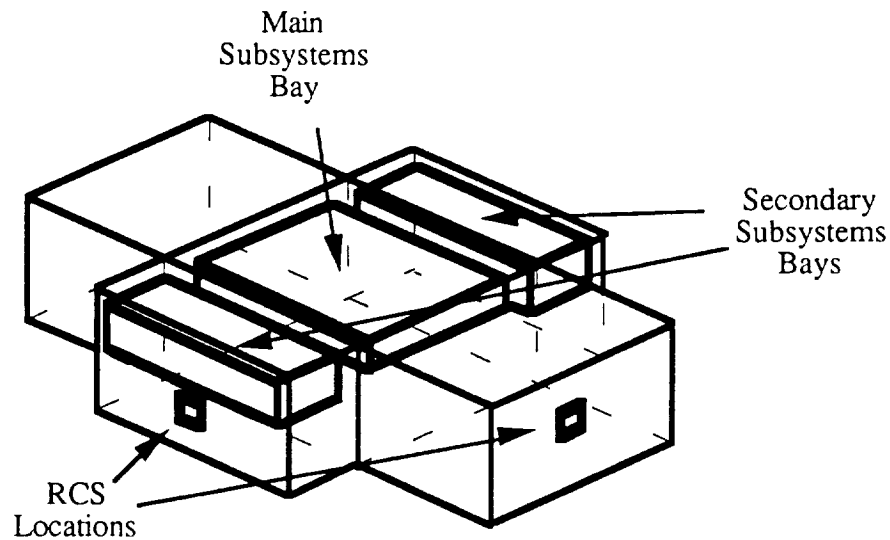


Figure 6.6 Subsystem Support

6.3 Landing Struts

The landing strut configuration chosen was an asymmetric four strut design (Figure 6.7). A four strut configuration was used to provide a maximum amount of stability while keeping the weight of the landing strut system to a minimum. An asymmetric type of strut configuration was used since the rails of the trolley system were incorporated into the forward landing struts. The forward struts were also extended to provide a larger moment arm to prevent the lander from tipping. This extension of the struts and trolley rail will leave the unloaded payload further from the engines, to minimize plume effects. The struts themselves are planar trusses (Figure 6.8) with lateral supports. These trusses offer little flexibility when loaded, therefore, a terrain adaptation system will be incorporated into the base of each strut. This system will allow approximately one meter of travel in each strut. A simple terrain adaptive system has been developed [12] and can be incorporated with a minimum of complexity.

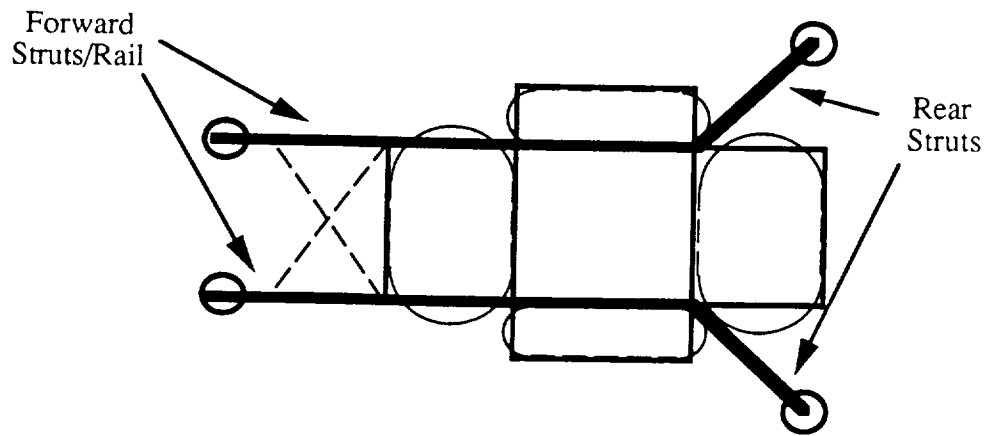


Figure 6.7 Strut Configuration

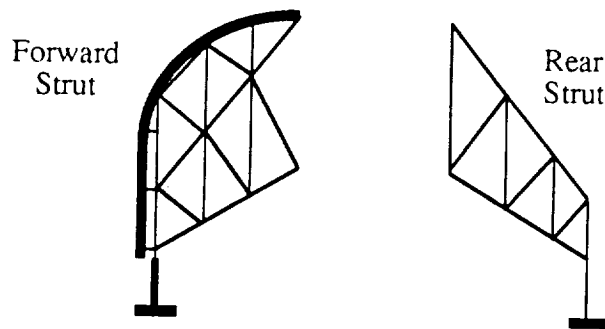


Figure 6.8 Landing Struts

If this terrain adaptive system is used, each landing strut will be equipped with a ground contact sensor and a brake/extension device. The sensor and extension device of each strut will be electronically connected to the central computer. During the touchdown phase of the landing sequence, the computer will unlock each extension device when its respective contact sensor has been activated. When the strut is unlocked, it is free to move. The lander will descend in a level attitude, until engine cutoff is initiated by the contact of all four pads. If the terrain variation under the lander is greater than that which can be compensated by the terrain adap-

tive system, the lander will continue to descend in a non-level attitude until contact of all four pads has been made.

6.4 Structure Materials

As stated earlier, the lander will be subjected to a variety of loads and stresses throughout its mission. Since the mass of the lander must be kept to a minimum, high performance materials should be used despite their higher initial cost. The weight savings will reduce propellant cost. Present composite material technology can provide materials with very high stiffness to weight ratios. Many of these materials are widely used in Earth based applications. However, the environment in space is far more demanding than on Earth. Typical fiber-reinforced composites would experience degradation after a reasonable exposure to the extreme vacuum and high temperature gradients in space [13]. Metal matrix composites can be made to survive in the space environment while providing high stiffness and high strength to weight ratios [14,15]. For special conditions, other materials could be used. If isotropic materials are specifically required, high performance aluminum or titanium alloys will be used. For ultra high temperature applications, such as turbines or combustion chambers, ceramic materials would be used. The use of these materials will maintain the overall structural efficiency of the lander.

6.5 Lander Construction and Assembly

The lander will be constructed on Earth and will be transported in modular form to the Space Station where it will be assembled. The multi-box structure of the lander will facilitate the lander's division into modules.

6.5.1 Modular Construction

The lander will be broken into five main components. These modules include the forward and aft tank boxes (H_2), the right and left tank/subsystem boxes (O_2), and the central engine/subsystem box. Each of these modules will be fully assembled and inspected on Earth. The modules will be sized to fit within the payload bay of the Space Shuttle and other future launch vehicles. Since the complete lander will not fit in the shuttle payload bay or other possible launch vehicles, modular construction is a necessity. Furthermore, partial construction in orbit can also save weight, since the landing struts will not support the lander in the Earth's gravity. Defective modules can be replaced or removed for repair quickly and easily even during an EVA on the lunar surface.

6.5.2 Assembly and Refurbishing

The final assembly and refurbishing of the lander will be performed while in orbit. Due to a person's limited dexterity and mobility while working in space, these tasks must be made as simple as possible while assuring structural and system integrity. Therefore, subsystem connections between the modules must be designed for easy coupling. The structural connections between modules must also be easy to fasten and disconnect when necessary.

7.0 Subsystems

The lander can be divided into several subsystems: propulsion; reaction control; power; guidance, navigation, and control; communication; and thermal subsystems. Each subsystem description will include requirements, design, and options.

7.1 Propulsion

This section will describe the propulsion system of the lander and the requirements used to determine the design.

7.1.1 Propulsion Requirements

The main engines of the lander were required to have the following qualities:

- High Isp (Specific Impulse)
- Throttability
- Restart
- Fuel commonality with RCS
- Redundancy for engine-out scenarios
- 10° gimbal range
- On-orbit refueling

The first requirement, high Isp, limits the field of choices to solid or liquid propellant systems. The gimbaling requirement was necessary to compensate for an inoperative engine and to account for different CM locations. The throttability, restart, and refueling requirements originated from the lander's reusability requirement. After all the requirements were

evaluated, a liquid propellant was the clear choice. A more detailed presentation of this analysis is presented in Appendix E.

7.1.2 Main Engine Design

This section discusses the critical design parameters of the engine design: propellant choice, number of engines, and final engine type selection.

7.1.2.1 Propellant Choice

Cryogenic hydrogen and oxygen were chosen as the propellants because of their high Isp. They were chosen for their history of reliability. Table 7.1 presents the performance characteristics of cryogenic hydrogen and oxygen rocket fuel [16,17].

Table 7.1: Hydrogen and Oxygen Performance Characteristics

Mixture Ratio by Weight	3.5
by Volume	.21
Average Specific Gravity, (g/cc)	.26
Chamber Temperature, (°F)	5870
Specific Impulse, (sec)	450
Ratio of Specific Heats	1.22
Bulk Density, (gm/cm ³)	.43

The liquid hydrogen and oxygen must be stored as cryogenic liquids to be used in the engines. The fuel tanks will be insulated to prevent boil-off. The tank volumes were determined from the ΔV requirements of the mission. The tanks used on the lander are cylindrical with hemi-spherical

endcaps and will contain baffles which prevent sloshing and add to their structural stiffness.

7.1.2.2 Number of Engines

The next process in deriving the propulsion system was to determine the number of engines required on the lander. Studies conducted by Aerojet, Pratt & Whitney, and Rocketdyne illustrated that three engines are favorable and most efficient based on failure analysis and weight concerns [16].

7.1.2.3 Engine Selection

Using the number of engines, mass, and ΔV requirements of the lander, calculations were performed to determine the maximum thrust required for the mission. This was found to be 54,629 lbs and occurred when performing a three 'g' landing (see Appendix F). Therefore, engines that can provide 30,000 lbs of thrust are needed to satisfy the criteria. This results in a thrust level of 60% for all three engines operating and 90% for two engines operating. A survey of available engine types yielded an engine with multiple restart capability. The engine performance characteristics are shown in Table 7.2.

Table 7.2: Engine Performance

Propellant	LO ₂ /LH ₂
Engine Cycle	Closed Expander
Thrust, lbf (vac)	30,000
Spec. Impulse, (sec)	477
Gimbal, (deg)	6 - 10
Chamber pressure, psia	1900
Mixture ratio (O/F)	6/1

Expansion ratio	200/450
Exit diameter, (in)	45/68
Length, (in)	63/126
Weight, (lbm)	1000

With the six to ten degree gimbaling capability, the center of gravity range can be seen in Figure 7.1.

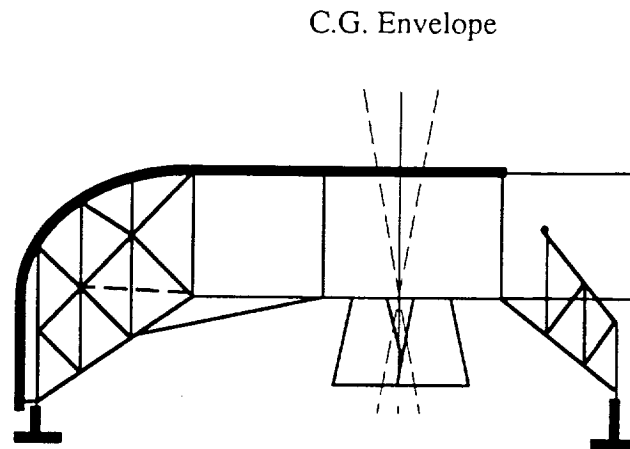


Figure 7.1 CG Range with 10° of gimbaling

7.2 Reaction Control System

The Reaction Control System (RCS) will be responsible for performing small course correction burns in orbit, and for attitude changes during the descent, ascent, and rendezvous phases of the mission. The system must be capable of providing translational and rotational control about the pitch, roll, and yaw axes.

7.2.1 RCS Configuration

The RCS will consist of a set of control modules, one on each of the four faces of the lander. Each thruster module will contain primary and

vernier thrusters that will be oriented in four different directions. (Figure 7.2). The location of each module will provide sufficient control about all three axes.

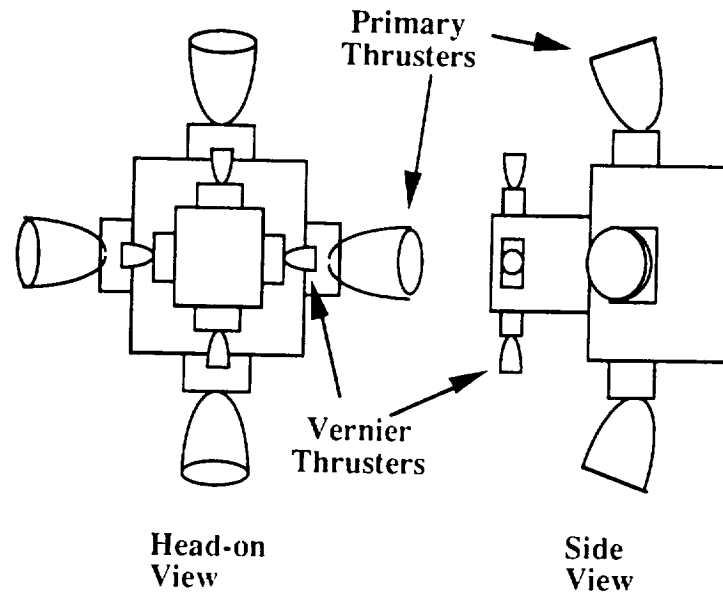


Figure 7.2 RCS Thrusters

7.2.2 RCS Propellant

Hydrogen (H_2) has been chosen for the fuel and Oxygen (O_2) has been chosen as the oxidizer for the RCS. This combination of fuels was selected for a variety of reasons. The major advantage of using H_2 and O_2 is that a high value of I_{sp} is possible, while minimizing the system mass. The RCS is refueled simultaneously with the refueling of the main propellant. Only two refueling ports will be necessary, one each for the H_2 and O_2 . Fuel and oxidizer will be transferred from the OTV to the main engine propellant tanks. Transfer from the main tanks to the RCS will be done internally. This configuration allows fewer locations for possible fuel and oxidizer spillage, increasing the overall safety of the system. Additionally, H_2 and O_2 produce relatively clean exhaust which is noncorrosive. The RCS noz-

zles will have lower maintenance requirements, thus, providing a more reliable system.

7.2.3 RCS Propellant Feed System

The actual RCS feed system is still to be determined, and will be dependent on the RCS technology advancements made in the next several years. There are, however, several features which will be essential to the system. A proposed RCS will consist of primary and vernier thrusters to provide large and small amounts of thrust respectively. The primary thrusters will require a set of accumulation tanks that contain liquid H_2 and O_2 for usage during the critical phases of the mission; namely, descent, landing, and OTV rendezvous. A schematic of a possible primary RCS is shown in Figure (7.3). Fuel and oxidizer will be bled off from the main tanks and transferred to the RCS accumulation tanks. High pressure turbo-pumps will feed the propellant through the system to the primary RCS jet combustion chambers.

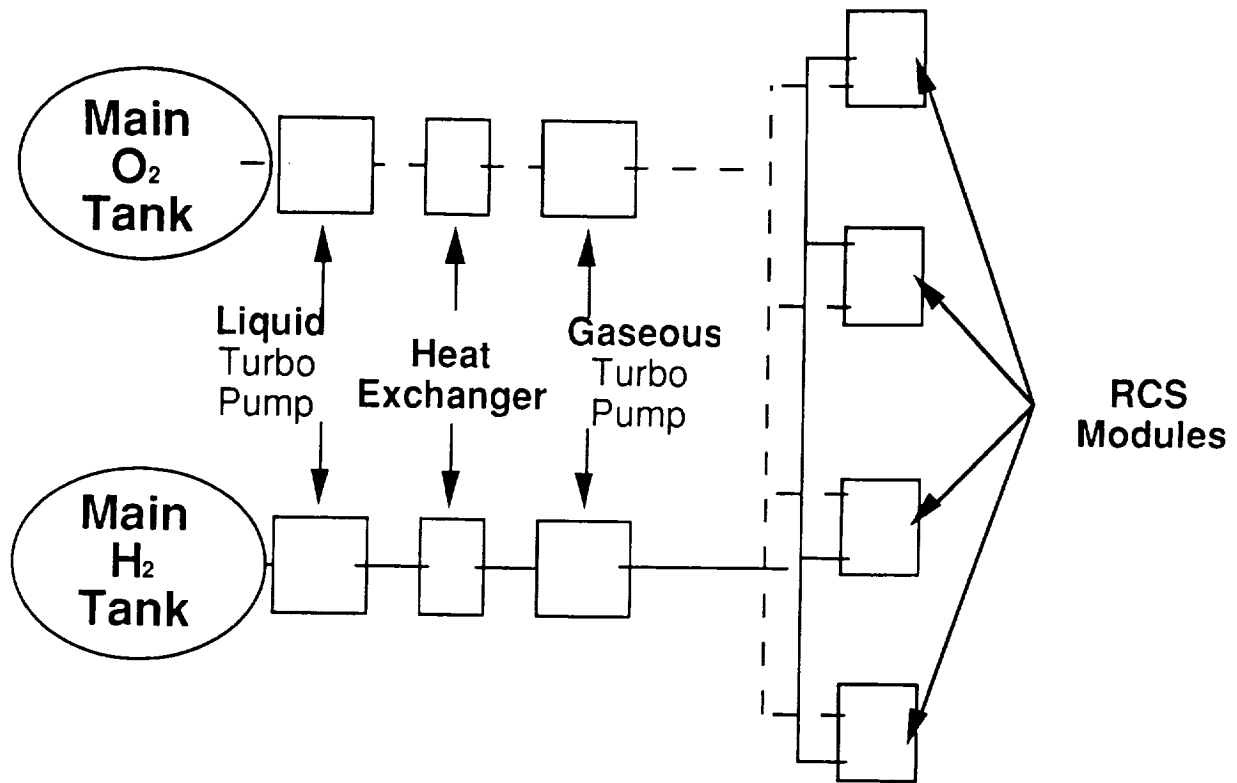


Figure 7.3 RCS Schematic

The vernier thrusters, however, will not need the set of accumulation tanks necessary for the primary thrusters. Since these engines will be providing relatively small amounts of thrust, the system will change the phase of the propellant from liquid to gas as the vernier thrusters are fired. The boil-off from the main propellant tanks might also be used to feed these engines. A schematic is shown in Figure 7.4.

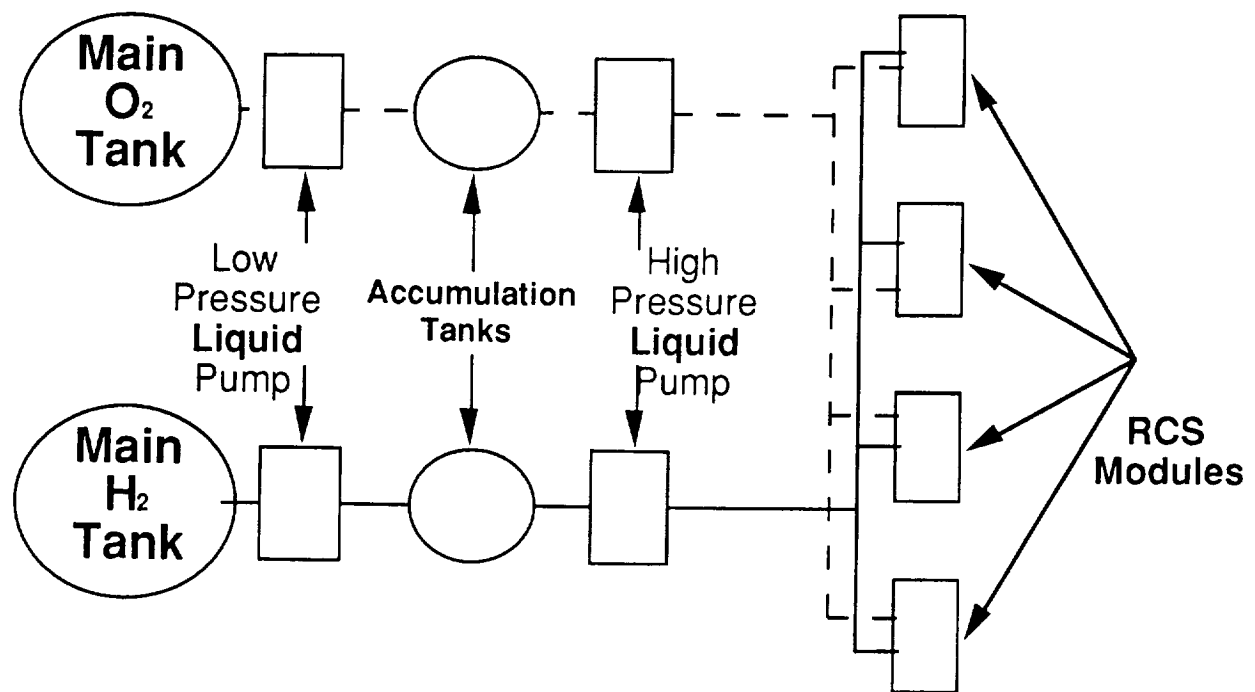


Figure 7.4 Vernier Thruster Schematic

Augmented spark ignitors will be necessary to initiate RCS firing. These initiators are capable of an unlimited number of starts which is a requirement of the RCS. One ignitor will be needed for each control thruster.

The RCS will provide sufficient thrust to perform small course corrections while in orbit and attitude changes during descent, landing, and rendezvous. The magnitude of thrust for the primary and vernier engines will depend on vehicle sizing and performance requirements.

7.3 Power Systems

The power subsystem will provide electrical power to operate all other lander subsystems. The following section discusses the power requirements of the lander, the power system itself, and the design decisions that lead to the power system.

7.3.1 Requirements

The lander has two operating modes: a constant, low power mode and a short duration, high power mode. The lander must be able to operate in either of these modes during day or night to prevent mission constraints. A summary of the power requirements for the various phases of the lander's mission is shown in Table 7.3.

Table 7.3 Power Requirements Summary

Active Mission Power Storage System	
NaS Batteries	92 kg (22 liters)
(includes thermal control)	
On Orbit Power Supply	
GaAs Photovoltaic Solar Arrays	
Structure	6.8 kg
Cells	3.3 kg (7.8 m ²)
Power Management and Distribution	0.6 kg
TOTAL	102.7 kg

7.3.1.1 On Mission Time vs. Off Mission Time

A typical mission lasts only 6 hours, but the time between missions can last from nine days to over three months if the OTV is delayed (Section 4.1). Since peak power usage occurs only for a short time during a mission, rechargeable power systems are advantageous.

7.3.1.2 High Power Mode

The highest power consumption occurs when the lander is in a mission during engine firing. The operation of the valves and the electro-mechanical actuators requires up to ten kW, but only for approximately ten minutes per mission. Other high power operations take place during the

mission, such as motor operation for the trolley and the retraction and deployment of the solar arrays. These operations require less than one kW and are also of short duration.

7.3.1.3 Low Power Mode

When in low power mode, only the basic subsystems of the lander are functioning. These subsystems include GN&C, communications, thermal control, and station-keeping RCS. Recharge of power storage systems would also occur in the low power mode. The lander is in low power mode while in its parking orbit between missions and for most of the mission except during engine firing, as discussed in the high power mode section.

7.3.2 Power Subsystem Hardware and Operation

The power system can be divided into two subsystems: an active mission power storage system and an on-orbit power supply.

7.3.2.1 Active Mission Power Storage System

The active mission power storage system is composed of sodium-sulfide batteries. These batteries provide enough power for the lander to complete a full mission and a full orbit in darkness before the on-orbit power supply, solar photovoltaic arrays, need to be used. Sodium-sulfide (NaS) batteries were chosen for their high energy to mass ratio and their rechargability. A TK-Solver model was used to compute the size of the batteries. This model is shown in Appendix G.

The specific weight, 12.5 kg/kWhr used for the NaS batteries includes the cells, primary battery, thermal protection and heat pipes [18]. This specific weight is very different from those given in other sources, which were

as high as 200 Whr/kg [19], but this value did not include the thermal systems for the NaS batteries. NaS batteries have a very high and sensitive operating temperature, and the weight of the thermal system for the batteries must be included for a reasonable estimate of the mass and volume. Because of their thermal sensitivity, these batteries and their radiators should also be placed on the lander so that they are shielded from the Sun.

The batteries have been estimated to have a mission life of 33 months, based upon a maximum of 2000 cycles [19]. The depth of discharge during peak power usage in the mission was limited to 80%. This produced a depth of discharge of 7.5% during on-orbit night power supply. This is also calculated in the TK-Solver model in Appendix G. Based on a maximum of three months between missions, the NaS batteries will last for the ten missions before lander is serviced.

7.3.2.2 On-Orbit Power Supply

Gallium-arsenic solar photovoltaic arrays are used to provide the on-orbit power supply when in view of the Sun. When the lander is operating in the Moon's shadow, the batteries are used as the on-orbit power supply. While in orbit, the solar arrays must be able to recharge the on-orbit night usage as well as the active mission power supply. This is reflected in the TK-Solver model used to size the arrays, as shown in Appendix C. To be conservative, it was assumed that the lander would be in night for one half of its orbit. Structural support, deployment booms, and radiator space were all included in the mass calculations [20].

Because the solar arrays are delicate structures that are susceptible to particle damage, the arrays are retracted before each mission and are

therefore protected from engine loads and lunar dust. The locations of the arrays, both when deployed and retracted, are shown in Figure 7.5.

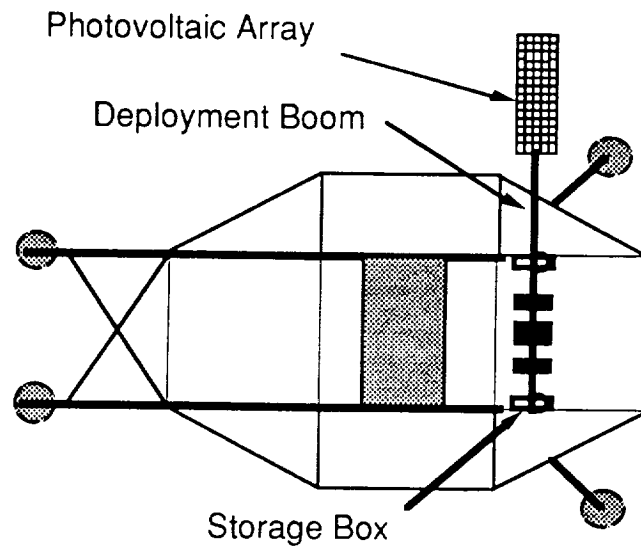


Figure 7.5 Photovoltaic Array Schematic

7.3.3 Power System Design

Several power systems available for smaller space vehicles were surveyed when determining the power systems for the lander. These included:

- Radioisotope Thermoelectric Generator (RTG)
- Fuel Cells
- Batteries
- Solar Photovoltaic Arrays

The primary design for the lunar lander power system was a combination of a chemical and solar power system. The chemical power system, either batteries or fuel cells, will provide for high and low power operation when not in sunlight. A solar power system will provide low power operation and chemical power system recharge when in sunlight.

The choice of a chemical power system depended upon a design study that considered weight, reliability, and re-use. The possible commonality of fuel for the propulsion system and for fuel cells was investigated for possible weight-savings.

The chemical power system will be required to supply enough energy to perform a complete mission in lunar night and supply the lander at low power until the solar system can recharge the stored energy.

7.3.3.1 Active Mission Power Supply Design

Fuel cells produce electrical power from the chemical reaction of fuels and oxidants which are stored externally to the cell. Regenerative fuel cells, which use a secondary source of power to regenerate the reactants from the waste products of the chemical reaction, are also being developed. Fuel cells are massive systems since they require the constant flow and storage of reactants such as hydrogen and oxygen, but these systems can provide power of around ten kW [21]. Current fuel cell technology provides systems with power densities of 20 kg/kW [22]. Problems with fuel cells include their low operating time of 10,000 hours, which has been improving. This is not within the expected mission life of the lander, but achievable with reasonable technological development [22]. Another problem with a fuel cell system is that each cell has a maximum load through which it can supply power. For the peak power consumption of the lander, the cell mass was over 200 kg. This mass was effectively wasted for the remainder of the mission.

Batteries produce electrical power directly from chemical energy and can also be recharged by a secondary source of electrical power. Batteries are massive-like fuel cells, but are very reliable even for rechargeable sys-

tems. Power output is up to 200 W hr/kg [19], but this does not include mass other than the primary cell. Nas batteries were chosen for their power to weight ratio and rechargability.

7.3.3.2 On-Orbit, Constant Power Supply Design

The two choices for the on-orbit power supply were the RTG and solar photovoltaic arrays. The RTG is a nuclear power unit that produces electrical power from the heat of the atomic decay of an element, usually Plutonium 238. The advantages of an RTG include long operating time and constant power supply without dependence upon the Sun. Disadvantages include the weight of the RTG and the required shielding from the radioactivity. The peak power provided by current RTG systems is less than 500 watts. The power to weight ratios of these systems are approximately 2.2 watts per kilogram [21].

Solar photovoltaic cells produce electrical power from the Sun's rays. The power output from a solar array is dependent upon the area of the array and the distance from the Sun. For the Earth-Moon system, the energy from the Sun is about 130 watts/ft² [21]. Photovoltaic arrays can convert this into electrical energy at a power to weight ratio of 100 watts per kilogram and a power to array area ratio of 130 kW per square meter [18]. Although delicate, solar arrays can be deployed, retracted, and are a lightweight source of constant power when a spacecraft is in the view of the Sun.

Solar arrays were chosen for their higher power to weight ratios compared to the high weight and radioactivity of RTGs.

7.4 Guidance, Navigation, and Control

The function of the guidance, navigation and control (GNC) subsystem is to determine and control the state of the lander, i.e., linear and rotational position, velocity, and acceleration. The GN&C subsystem of the lander will be designed according to the proposed mission: deorbiting from rendezvous with an OTV to a predetermined site on the Moon. It is assumed that there will not be manned presence, transponders, or receivers on the lunar surface to assist in navigation. However, the lander must also be designed to take advantage of a lunar base and any transponders or receivers that may be used there in future missions. The GN&C subsystem can be divided into many components, the most important of which are:

- Inertial Guidance
- Navigation
- Control
- Data Processing and Management.

Figure 7.6 shows a schematic indicating the interaction among components of the GN&C subsystem and Figure 7.7 is a block diagram description.

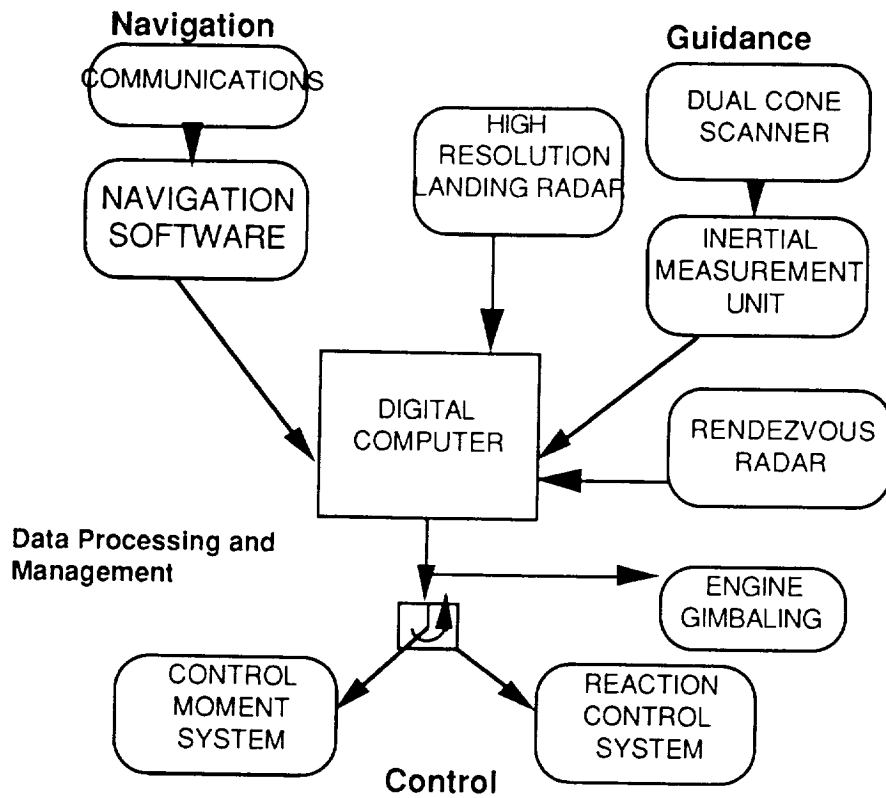


Figure 7.6 GN&C Schematic

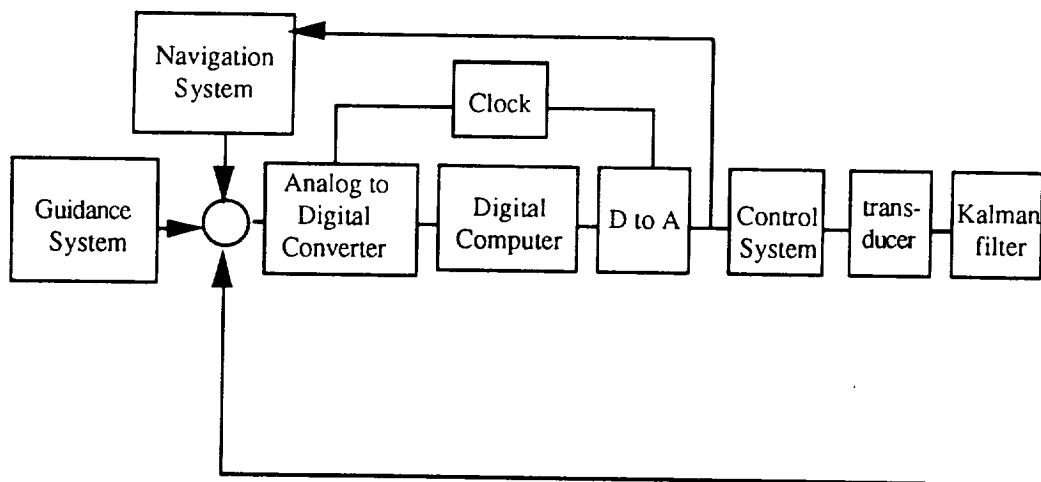


Figure 7.7 GN&C Block Diagram Description

7.4.1 Inertial Guidance

The guidance system will be quadruple redundant and will provide the computer with continuous attitude, position, and rotation information. The major components of this system will be a Dual Cone Scanner, an Inertial Measurement Unit (IMU), as well as rendezvous and landing radar.

Two Dual Cone Scanners with Sun Fans will be used to update attitude and orbit determination periodically. The Scanners will provide all orbital parameters and attitude information. Updates will be required particularly after burns and during ascent and descent. The Scanner is a device used to calibrate the IMU and provide orbital position information for distances far from the Moon.

Two Inertial Measurement Units will be used to provide continuous orbit determination in inertial coordinates. This system uses initial conditions from the Scanner because it loses accuracy over time. The IMU consists of three laser rate gyros with three accelerometers to provide all attitude information. Recent missile guidance technology provides IMU's of negligible mass and power requirements [23].

For landing on the lunar surface, a high precision radar system will be required in order to avoid obstacles, such as boulders or craters, and land on a level surface. This will include a terrain imaging device and obstacle avoidance software for determining the final landing position.

A separate system will be required for rendezvous and other proximity operations. This Rendezvous Radar system will consist of X band radar with rendezvous transponders located on the OTV and the lander, which will provide accurate range and range rate measurements necessary for rendezvous with the OTV. The same system at a different operating frequency may be used for landing at a lunar base.

7.4.2 Navigation

The navigation system is directly in line with the communications subsystem and the central computer. This system will consist of software as well as a positioning system to allow for real time or near real time control of the lander.

The navigation software will be an operational map for the lander and will be run on the central computer. The computer will track the state of the vehicle from the IMU's and downlink it to Earth periodically, which will allow for Earth based command signals to change or correct the pre-programmed mission.

If real time control will be required for operations on the far side of the Moon, then a Lunar Positioning System will be required for lunar approach navigation. This system uses a minimum of three satellites to allow for real time control at any position on the Moon. Four satellites will be required to include polar positioning. If frequent far side operations will not be performed, e.g., for a far side lunar base, then the Global Positioning System may be used to provide continuous, real time positioning for near side operations. This would be the lower cost alternative for lunar approach navigation. The positioning system will provide orbital location information as the lander approaches the lunar surface.

7.4.3 Control

Attitude Control will be performed redundantly by a Control Moment System (CMS) and a Reaction Control System (RCS) which are in direct line with the central digital computer. Control of CM changes will be provided using thrust vector control (TVC).

The CMS consists of Control Moment Gyros (CMG) which are used to provide a change in attitude without external forces. This method of attitude control provides savings in fuel when only relatively small attitude changes are required. The system consists of three mutually perpendicular axis gyros with large enough mass to provide the required momentum changes. This system is useful for proximity operations.

The RCS System consists of two sets of four quadruple reaction control thrusters placed at symmetrical locations on a horizontal axis of the spacecraft (Section 7.2.1). These will be used when larger attitude changes are required or to dump off angular momentum in the case that the CMGs reach maximum speed and the lander remains in a fixed, undesired attitude.

Thrust vector control will be provided by a ten degree gimbaling capability for each engine. This will correct for unstable CM locations and motion and instabilities due to the asymmetry of the lander.

7.4.4 Data Processing and Management

A computer such as a Barnes 1750A Processor will form the basis of the lander's avionics system, keeping track of the state of the spacecraft at all times and allowing for interface from ground control. This processor will combine the information from all GN&C systems for closed loop feedback control as well as integration of the state vector. An array of software will be used to map out the mission for the lander and check for any errors in operation. This digital system will be the interface among the GN&C components as well as the point of interaction for Earth based control. Connection of the different components will be achieved by the use of a fiber-optic "fly-by-light" system for maximum reliability and signal clarity,

as well as minimum weight and power requirements. A redundant computer system will be required for backup in case of computer malfunction [24].

7.5 Communication

The lunar lander mission requires four different communication links: lander-OTV, lander-Earth, lander-lunar base, and Earth-OTV, the first three of which will be considered in this project. The Earth-OTV communications will be left to the design of the OTV. These will be considered only in the fact that communication between the lander and the OTV must be at a different frequency than that between the OTV and Earth. Earth communications will be provided through the use of the advanced Tracking Data Relay Satellite System (TDRSS) or Tracking Data Acquisition System (TDAS) system. Thus, in this section, communication with Earth will refer to communication with TDAS.

7.5.1 Lander-Earth Communications

For near side operations the lander will have direct communications with an Earth based command center. This will include a periodic downlink of mission data, including the state of the lander and any system errors that may have occurred. In addition, command signals will be uplinked to the lander to make changes or corrections to the mission. This communication link will be provided by a radio transmitter with an amplifier using a steerable S-band antenna requiring 15 Watts of power. In the case that the S-band is overcrowded at the time of the mission, another appropriate bandwidth must be chosen for this line of communication. The antenna pointing direction will be determined using infrared sensors

which detect the infrared signature of the Earth. This system is partially based on a similar system used on the Apollo spacecraft [25].

7.5.2 Lander-OTV Communications

The need for communication between the lander and the OTV is twofold. The first purpose is for interaction during docking and refueling. This will be required for the complex procedure of aligning the two vehicles to make a safe connection. Furthermore, the two must communicate in the case where the lander is on the far side of the Moon and communication is required between the lander and the Earth. Thus, if there is a system malfunction during far side operations, the lander can send a signal to the OTV, and the OTV, in low lunar orbit, can convey the message back to Earth. Likewise, if a change in the mission is desired, Earth control can send a signal to the OTV, which can orbit to the far side and relay the message to the lander. For the lander-OTV communication, an X band radar antenna will be used for sending and receiving range and range rate information for proximity operations. A low power VHF antenna will be used for sending and receiving required data for Earth bound communication.

7.5.3 Lander-Lunar Base Communications

For later missions, upon construction of a lunar base, the lander will be required to have a communication link to the lunar base. For this short range communication, the low power VHF antenna will be used at a different frequency than that used for communication with the OTV.

7.6 Thermal Control System

The thermal control system will be responsible for dissipating the heat generated from the lander's subsystems. Due to the working in a vacuum, an active thermal control system was chosen for the avionics and the batteries. Passive systems are more attractive in terms of mass and power requirements, but they do not provide the protection for all systems. These passive systems will be used for the thermal protection of the cryogenic fuel.

The active thermal control system chosen is similar to the cold-plates used on the Space Shuttle. These cold-plates are simply flat pallets that contain plumbing running through them. A working fluid such as Freon is pumped through these lines to lower the temperature of the plate. The item to be cooled will be bolted to the cold-plates, and heat will be transferred from the item to the working fluid by means of conduction. The heat is then vented through a radiator which is in the closed-loop system (Figure 7.8).

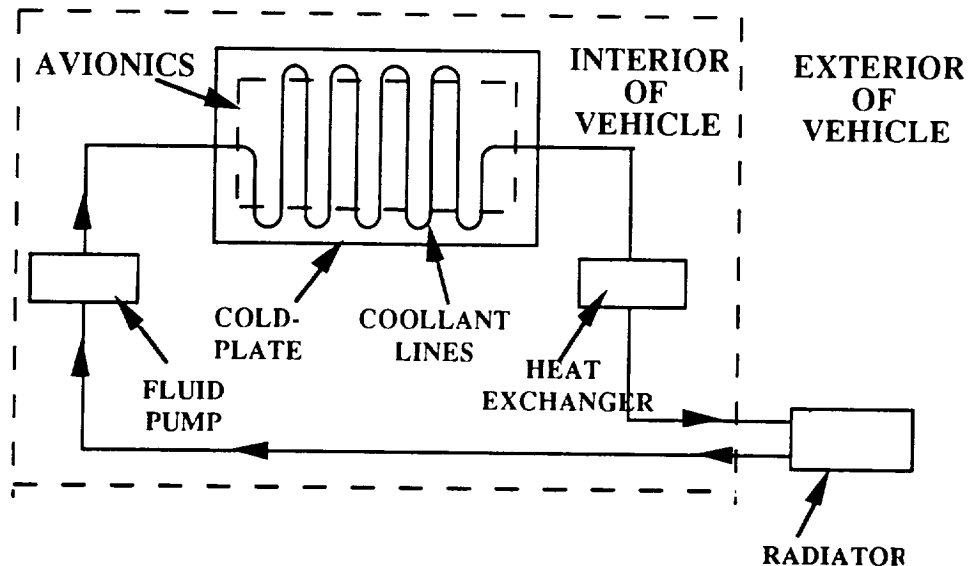


Figure 7.8 Cooling System Schematic

This type of thermal control will be easily implemented since all of the avionics will be housed in a single storage area. A set of cold-plates will be mounted into the avionics bay, and the avionics equipment will then be bolted directly onto these plates. Other systems that are temperature-sensitive are the batteries and the propellant tanks. The NaS batteries require heat exchangers and radiators also, and the weight of these systems is included in the battery weight [18]. Sensors will be used to keep the equipment within a specified range of temperatures.

Other systems will be cooled by passive means. The temperature of the cryogenic fuels must be controlled to prevent excessive boil-off of the fuel. Boil-off will be limited by the maximum time that the tanks will be full, 14 days. The boil-off that will occur will not be wasted since it can be used by the gaseous H_2/O_2 RCS thrusters for station-keeping. Even so, the boil-off will be minimized by insulating the propellant tanks and shielding them from direct sunlight by an intervening structure.

Problems occur when choosing the working medium for the system. The Space Shuttle uses Freon-21. This fluid works very well, but there is a reliability problem since the system needs refurbishing after every flight. The lander is required to perform a minimum of ten missions, so Freon would not be a prudent choice. The ultimate selection of the actual working fluid is yet to be determined and is dependent of the technological advances in this area in the near future.

In order for the radiators to remove heat efficiently, they should be kept out of the Sun. All radiators are on the top side of the lander and this side will be kept out of the Sun when the lander is in its parking orbit. The radiator placement will protect them from lunar dust blown by the plume of the rocket engines.

8.0 Requirement Changes

Certain factors of the design of the self-unloading reusable lunar lander influenced the decision to change some of the original requirements given by the RFP. These requirements stated that the lander must be capable of carrying the mass of the unloader plus the payload and that the unloader should be able to unload its own mass plus the payload. Other requirements stated that the lander would have the capability to return to LLO without the unloading device.

8.1 Light Fixed Unloader

The trolley system is permanently attached to the lander. Although the RFP seemed to require a detachable and autonomous unloader, we determined this would make the lander too complex and heavy. The fixed unloader design was selected for its simplistic, lightweight design. For this reason, the RFP requirements of a detachable unloader were changed.

8.2 Increased Payload

Because our design does not include a detachable unloader, the payload weight was increased from 7,000 kg to 15,000 kg. The trolley system will weigh much less than a detachable unloader since it is light and integrated into the system. It was believed that a detachable unloader would weigh approximately the same amount as the payload. For this reason, the payload mass was doubled and then increased to 15,000 kg to give a more practical figure.

9.0 Reusability

One of the most demanding and important of the lander's requirements is the ability to perform ten missions between servicing. Operating remotely at the Moon, the lander must be able to perform its mission without needing a costly boost back to LEO.

With this in mind, the lander is designed to be reusable and reliable. Present day technology and conservative technology forecasts were used. The lander is designed and systems are located to minimize the hazardous effects of the lunar environment. Simplicity was a major goal. An unloader with a minimum number of moving parts was chosen. A common fuel and oxidizer were used for the main engines and RCS to simplify refueling.

Once the lander has completed ten missions, it is not meant to become another piece of space debris. Modular construction will allow astronauts to replace pieces of the lander in orbit, from propellant tank modules to an avionics package. Ideally, the lander will spend a minimum amount of time at an orbital workshop in LEO for systems check and battery replacement before being sent back to duty on the Moon for another ten missions.

10.0 Technology Development

Because the lunar lander mission will probably occur sometime after the year 2000, some aspects of the lander were designed according to recent or projected technology in spacecraft operations and subsystems. This section describes some areas in which the technology exists but direct applications have not been tested yet.

10.1 Hydrogen-Oxygen RCS Fuel

In the past, it has been a common practice to use separate fuels for the RCS system and the main engines. This is common because it has generally been desirable to have hypergolic fuel for RCS motors, which provide fast reaction time without a required ignition device. Cryogenics have been used for fueling the main engines in order to have a higher I_{sp} and thus a more efficient use of the fuel. However, for the lunar lander mission, liquid H_2/O_2 will be used for both RCS and main engines. This method has not been used in previous space missions, but it will be required in order to simplify the complex refueling procedure. Hypergolic fuels are a safety hazard and very corrosive. In addition, the lander needs the efficiency of the H_2/O_2 fuel. It is hoped that common fuel tanks will also save mass.

10.2 Automated Docking and Refueling

Automated docking and refueling have long been proposed space operations but have yet to be performed by United States spacecraft. The U.S.S.R., however, has successfully performed this task. The lunar lander mission must have this ability as well. The lander must function without a manned presence and the lag time for Earth communication is too long for complex maneuvers such as docking.

10.3 Advanced Artificial Intelligence

Many of the operations in the lander's mission will require some sort of artificial intelligence. Some of these include docking, refueling, and landing with an obstacle avoidance system. Expert systems will be necessary because these operations must be pre-programmed tasks in the mission software. Due to the lag time in communications from Earth to the Moon (about 4 seconds), most operations must be performed without any manned oversight or control.

10.4 Inertial Measurement Units

Recent technology provides IMU's with negligible mass and power requirements. These are currently projected for use in missile guidance systems. The miniature devices provide all attitude information with a slight loss in accuracy per current technology. However, over a ten year period, it will be assumed that the accuracy of the modern IMU's will surpass that of such systems in the past.

10.5 Tracking Data Acquisition System

Presently, spacecraft that leave Earth orbit communicate to Earth using the Deep Space Network (DSN). This system is geared for deep space probes and not the high demands of multiple manned craft. The present communication system for manned spacecraft, the Tracking Data Relay Satellite System (TDRSS), is not able to communicate with spacecraft outside of Earth orbit. Future space exploration demands a new system to handle communication for multiple vehicles outside of Earth orbit, and the system to fulfill this function is the Tracking Data Acquisition System

(TDAS). TDAS, the planned successor to TDRSS, should be able to handle communications with multiple landers, OTV's, and other craft throughout the solar system and relay this information to operators on Earth.

10.6 Increased Cooling System Mission Life

The cooling system used by the lander, a cold plate/radiator system, is similar to that used by the shuttle. However, the shuttle's system must be refurbished after every mission, but the lander must operate for at least ten missions before any repairs or replacement can occur. The mission performance of this system is adequate, but an increased mission life must be developed for use on the lander and other space vehicles operating without the benefit of Earth-based repair.

11.0 Mass Statement

The total wet mass of the lander before descent is 49376 kg. This mass includes 9790 kg of inert mass, 24586 kg of propellant, and 15000 kg of payload. The masses of the various subsystems are based on reference [17]. The structural mass is scaled from the structural mass Apollo. The structural mass of the Apollo descent stage and landing gear was 842 kg. The total mass of the Apollo ascent stage, including ascent propellant mass, was 4535 kg. This ratio of payload mass to structural mass suggests that the structural mass of our lander should be 2785 kg (based on a payload of 15000 kg). Due to the fact that our lander is reusable and single staged, this mass was multiplied by a factor of 1.5, resulting in a total structural mass of 4180 kg (excluding the trolley system). The Trolley system is estimated to be an additional 200 kg. Table 11.1 lists the mass break down of the lander.

Table 11.1 - Mass Statement

Item	Mass (kg)
PAYLOAD	15000
INERTS	
Structure	4380
(Lander 4180)	--
(Trolley 200)	--
Engines	1360
RCS Dry	500
Propellant Tanks	2850
Electrical Power	100
GN&C	400
Data Processing System	50
Communication	100
Thermal Control	50

TOTAL INERT MASS	9790

PROPELLANT	
Descent	17930
Ascent	5756
RCS	900

TOTAL PROPELLANT MASS	24586
	=====
DEORBIT GROSS MASS	49376

12.0 Management Structure

The organizational structure of B&T engineering is broken down into three management levels and two independent branches (Figure 12.1). At the top of the organization is the project manager and directly beneath are the managers of the Engineering and Operations branches. All members of B&T engineering serve under both branches and make up the third management level. The Design/Operations division (within the Operations branch) is assigned the task of brainstorming conceptual designs, mission scenarios and assumptions, and identifies technical tasks to be completed by the Engineering branch. In order to be as adaptive as possible, the branch managers can appoint temporary leadership roles to any engineer, so that a particular conceptual or technical task may receive special attention.

The organizational structure ensures efficiency by evenly distributing the work load among all engineers and provides an opportunity for each engineer to be engaged in conceptual as well technical tasks. These objectives are accomplished by allowing each engineer to work concurrently in the Operations branch and the Engineering branch.

During the Preliminary design phase of the lunar lander project, the main concentration was within the Design & Operations division. This area was emphasized in order to come up with the best overall lander/unloader concept. After the selection of the overall concept, the emphasis of the work was shifted to the various technical groups. The technical groups continued to interact to complete the remaining design tasks within the project's allotted time.

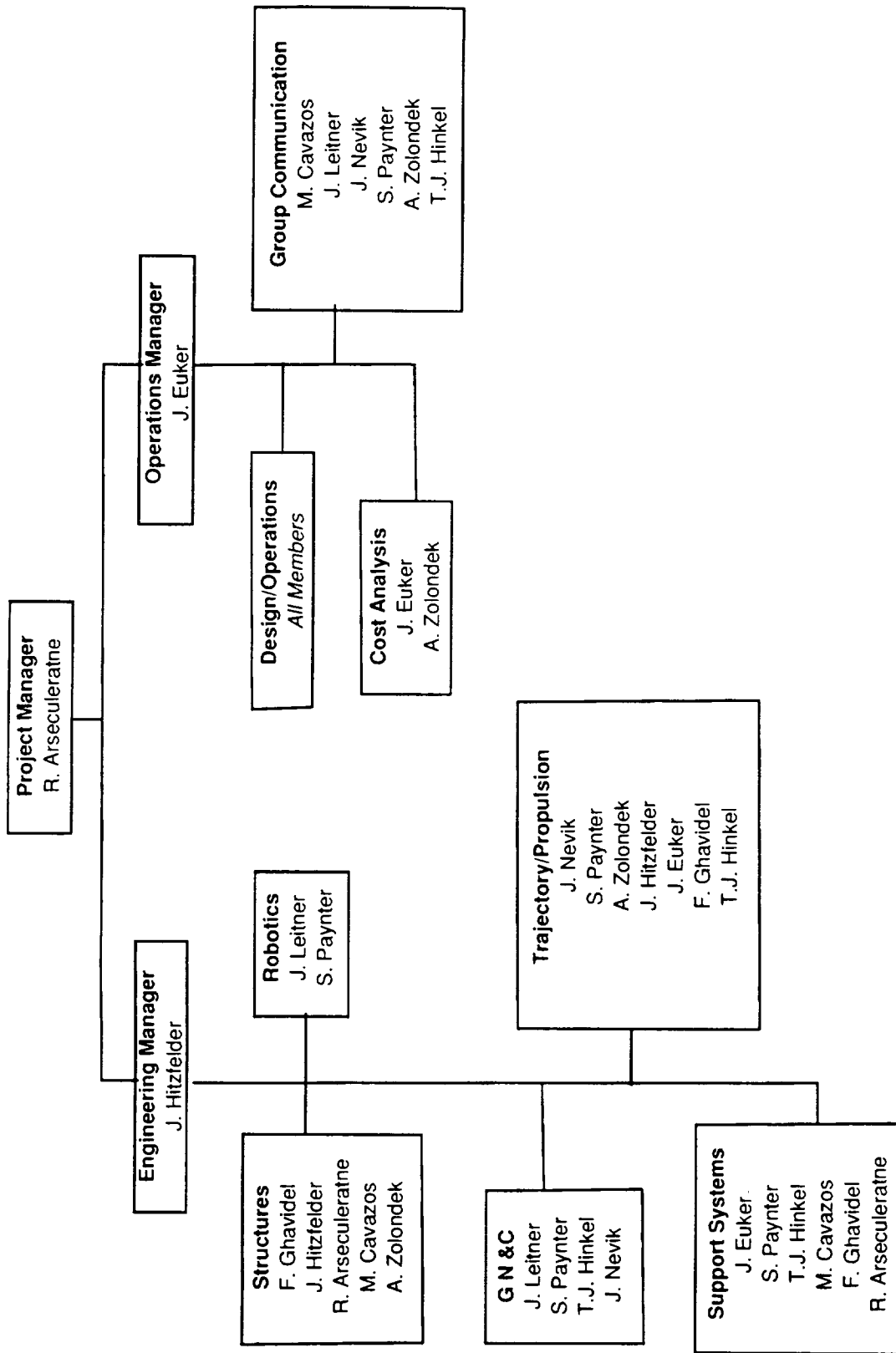


Figure 12.1 Management Chart

12.1 Managerial Communication

Since B&T Engineering is comprised of a relatively large group, communication between members is crucial in maintaining efficiency and productivity. The lines of communication among members are depicted in Figure 12.2 and are briefly described below.

- The Project manager sets the pace and the agenda for the whole group. His inputs feed directly to the Operations manager and can also feed forward to the Engineering manager.
- The Design/Operations group meetings provide an arena for discussion and feedback on mission concepts. The Design/Operations group informs the Engineering manager of tasks to be accomplished by the Engineering division.
- The Engineering manager provides the connectivity between each separate technical group and ensures the compatibility of all technical solutions.
- The feedback paths from the Engineering and Operations groups are formed by the reporting of individuals during the Operations meetings, by meetings between the Project manager, and the two branch managers.

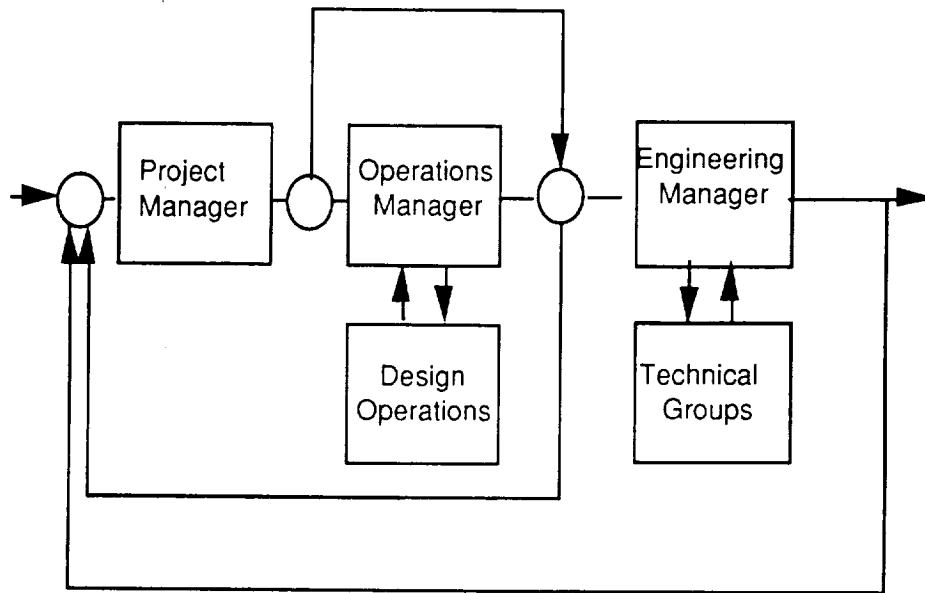
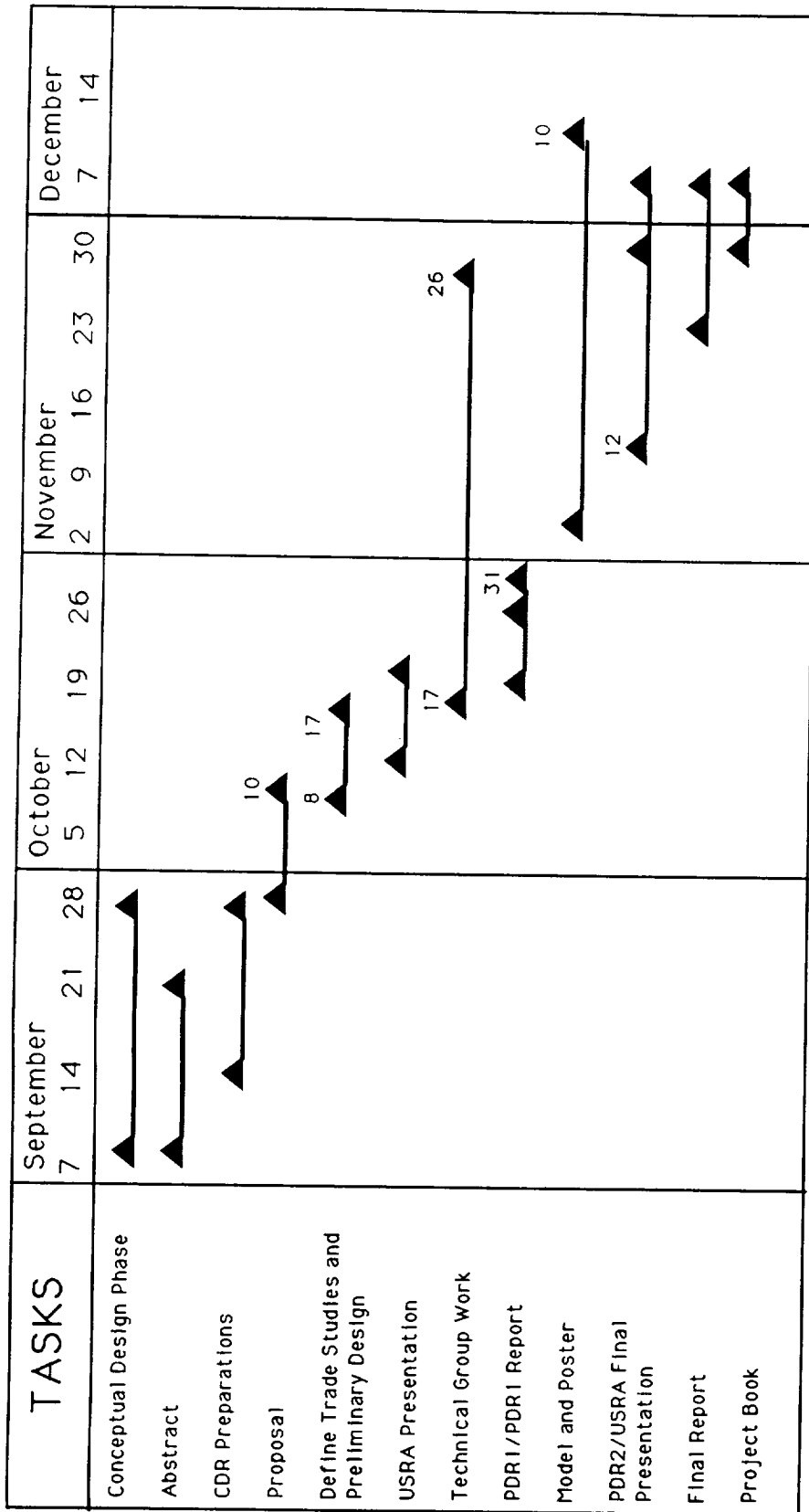


Figure 12.2 Project Communication Schematic

Since there are many avenues by which problems can be reported, they can be dealt with quickly. For instance, if a technical problem were to arise, the difficulty would first be dealt with within the Engineering branch. If the problem cannot be resolved within the Engineering branch, the Engineering manager and the engineers working on the problem will bring this to the attention of the Project manager and the Operations manager. If it is found that this dilemma can only be corrected by a change in an overall concept or scenario, it will be brought to the Design/Operations group for consideration.

12.2 Program Schedule

The preliminary schedule of the Self-Unloading Reusable Lunar Lander project was presented in the Proposal. This schedule is depicted in a Gantt chart in Figure 12.3. With the exception of a few delays, the project was completed by the time originally projected.



▲ Set Dates

△ Flexible Dates

Figure 12.1 Gantt Chart

13.0 Cost

The costing methodology used for this contract is based on estimating personnel, supply, and computer costs. All three categories are estimated from the amount of work performed to date on the contract.

13.1 Personnel Costs

The hourly wages for the various levels of personnel are based on the hourly wages of previous studies. The number of hours per week are based on a total group meetings time of 5 hours per week and an additional 10 hours per week of individual time.

	Hourly	Hours per	Weekly	16Week
Personnel Costs	Wage	Week	Salary	Salary
1 Project Manager	\$ 25	15	\$ 375	\$ 6000
1 Technical Manager	22	15	330	5280
1 Operations Manager	22	15	330	5280
7 Engineers	20	15	300	33600
Consultants	75	2	150	2400
Subtotal				\$ 52560
Plus 10% error estimate				5256
Total Personnel Cost				\$ 57816

13.2 Supply Costs

The costs of the various categories were calculated as follows. The number of photocopies required was estimated at 800. The number of transparencies required was estimated at 100 (5 presentations x 20 viewgraphs). The categories of long-distance calls, model, and poster/display are estimated from experience on other contracts.

Supply Costs	16 Week Total
Photocopies (\$0.06 each)	\$ 48.00
Transparencies (\$0.50 each)	50.00
Long-Distances Calls	100.00
Model	50.00
Poster/Display	50.00
Subtotal	\$ 298.00
Plus 10% error estimate	29.80
Total Supply Costs	\$ 327.80

13.3 Computer Costs

The computer costs are based on four months rent of both Macintosh and IBM computers. The costs reflect the emphasis on Macintosh computers.

Computer Costs	16 Week Total
4 Months Rent Macintosh/Peripherals	\$ 1500.00
4 Months Rent IBM/Peripherals	800.00
Subtotal	\$ 2300.00
Plus 10% error estimate	230.00
Total Computer Costs	\$ 2530.00

13.4 Total Contract Costs

The total cost associated with the completion of the contract for the design of a self-unloading reusable lunar lander is \$60,674 (1990 dollars).

Total Contract Costs	16 Week Total
Personnel Costs	\$ 57816
Supply Costs	328
Computer Costs	2530
Grand Total	\$ 60674

14.0 References

1. Bate, R.R., Mueller, D.D., and White, J.E., Fundamentals of Astrodynamics. New York: Dover Publications, Inc., 1971.
2. Chris Varner, Eagle Engineering, Inc. Interview, November 16, 1990.
3. "Mixed-Vehicle Transportation Fleet for Mission to Lunar Polar Orbits," Austin, Texas, Paper No. LBS-88-198, 1988
4. NASA, "Space Shuttle Press Release." U. S. Government Printing Office.
5. Tim Thornton, Ford Aerospace Operations. Interview, November 2, 1990.
6. Newkirk, Dennis, Almanac of Soviet Manned Space Flight. Houston: Gulf Publishing Co., 1990.
7. Tillman, Marc et al., Project ARGO. Ann Arbor: The University of Michigan, 1989.
8. Nishimura, Makoto et al., "Lubrication Properties of Molybdenum Disulfide Films Deposited by RF Sputtering Method." Tokyo: National Aerospace Laboratories, 1986.
9. Carrier, D.W., Olhoeft, G.R., and Mendell, W., "Physical Properties of Lunar Surface." Houston: Lunar Planetary Institute (unpublished).
10. Hernadez, C.A., Sunder, S., and Vestgaard, B., Design of a Thermal and Micrometeorite Protection System for an Unmanned Lunar Cargo Lander. Austin: The University of Texas at Austin, 1989.
11. de Ste. Croix, Philip, Editor, Space Technology. New York: Crown Publishers, Inc., 1981, pp. 160-7.
12. Rivellini, Tommaso, et al., Lunar Polar Coring Lander. Austin: The University of Texas at Austin, 1990, pp. 45-6.
13. Dursch, Harry W., "Protective Coating for Composite Tubes in Space Applications." *SAMPE Quarterly*, Vol. 19, No. 1, October, 1987, p.14.
14. "Tensile Properties of Titanium Carbide Coated Carbon Fibre Aluminum Alloy Composites." *Composites*, Vol. 20, No. 5, September, 1989, p. 471.

15. "NASP Researchers Forge Ahead with Propulsion and Technical Advances." *Aviation Week & Space Technology*, Vol. 133, No. 18.
16. "Lunar Lander Conceptual Design," Eagle Engineering, Inc., Houston, Texas, EEIReport 88-181, March 30, 1988.
17. "Aeronautical Vestpocket Handbook," United Technologies Pratt & Whitney, Canada, August 1986.
18. "Space Power Systems Technology for the Manned Mars Mission" - Presentation Slides. Ann Arbor: University of Michigan, January 22, 1986.
19. McCusker, Todd, "Subsystem Reports: Propulsion Subsystems Reports and Database." Austin: The University of Texas at Austin, 1989.
20. "Space Power Systems" - Presentation Slides. Ann Arbor: University of Michigan, February 9, 1987.
21. Air Command and Staff College, Space Handbook. Maxwell AFB, Alabama: Air University Press, 1985.
22. Appleby, A.J. and Foulkes, F.R., Fuel Cell Handbook. New York: Van Nostrand Reinhold, 1989.
23. Deyst, J., Elwell, J., and Womble, E., "Guided missiles the size of baseballs and guidance systems that will fit in the palm of your hand are on the way." *Aerospace American*, Vol. 28, No. 10, October, 1990.
24. EDO Corporation, Barnes Engineering Division, "Dual Cone Scanner Specifications." Shelton, CT: The EDO Corporation, 1989.
25. Kayton, "Avionics for Manned Spacecraft." *IEEE Transactions on Aerospace and Electronic Systems*, Vol. 25, No. 6, November, 1989.

Appendix A: Design Process

This section presents the design process, from the preliminary concepts to the selection of the primary design. As shown in Figure A.1, the design process began with four preliminary concepts for the lander and unloader. From these four concepts, the Fixed Unloader was chosen as the preliminary concept. Five variations of the Fixed Unloader were then developed, as shown in the second level of Figure A.1. After choosing two of these variations, the ramp unloading variation was developed into the Trolley design, and the bottom unloading variation was developed into the Donut and Plunger designs. Using a decision matrix to evaluate these three designs, the Trolley design was chosen as the primary design for further development.

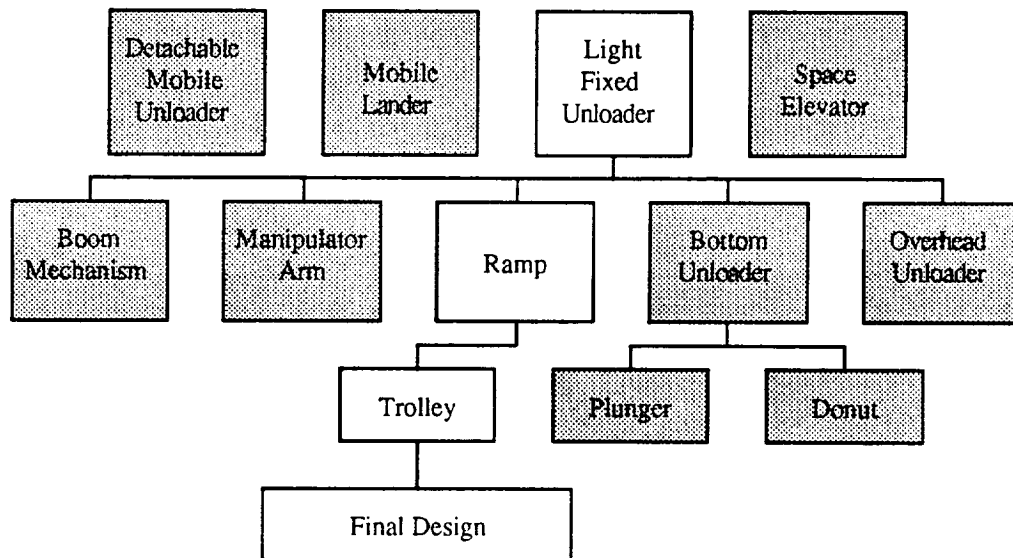


Figure A.1 The Design Process

A.1 Selection of Preliminary Concept

Four preliminary concepts were considered for the overall project mission. The concepts considered were: the Space Elevator, the Mobile Lander, the Detachable Unloader, and the Fixed Unloader.

A.1.1 Descriptions of Preliminary Concepts

The following sections give brief descriptions of the preliminary concepts and point out their strengths and weaknesses.

A.1.1.1 Space Elevator

The Space Elevator uses a tether to transfer payloads to the lunar surface. As shown in Figure A.2, the Space Elevator consists of a tether with one end anchored at the lunar surface and the other end attached to a docking module, which would be in lunar synchronous orbit. The tether would be gravity gradient stabilized. For a typical mission, the OTV will rendezvous with a docking module attached to the tether at the Lagrange point. The payload is transferred to the tether, and then lowered to the surface after an initial 'kick' is provided to start the payload moving. The rate of descent is controlled by a motorized payload/tether interface system. This system could also transfer payloads from the surface to the OTV.

The main advantage of the Space Elevator is that less fuel is required for ascent, descent, and rendezvous.

The biggest disadvantage of this system is the length of the tether. The Space Elevator requires a tether 60,000 km in length, resulting in an enormous weight. Another major disadvantage of this system is that the payloads can only be delivered to a single location on the lunar surface.

Additionally, a system to anchor the tether to the lunar surface must first be landed on the surface before the Space Elevator can be constructed.

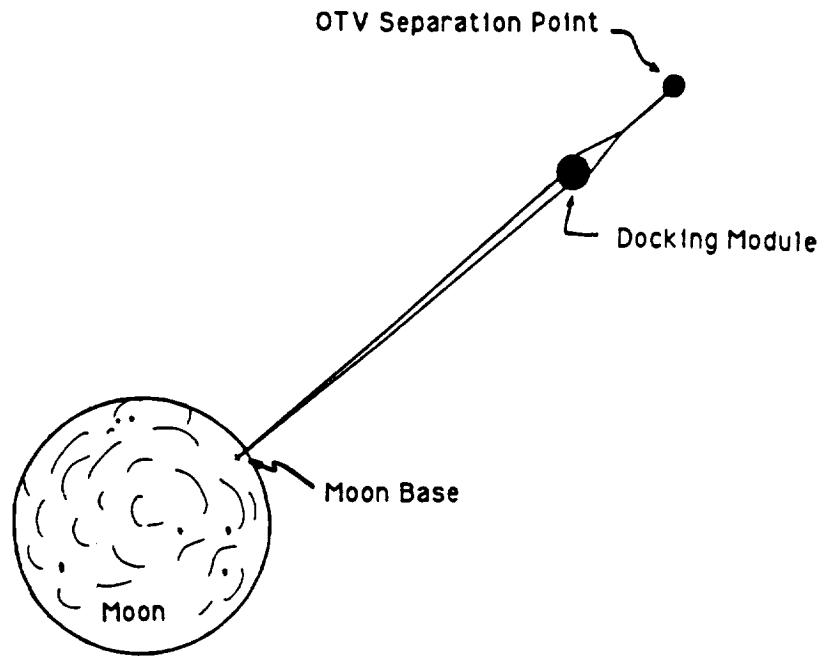


Figure A.2 The Space Elevator

A.1.1.2 Detachable Unloader

The Detachable Unloader concept consists of two separate vehicles, the lander and the unloader. After landing, the unloader detaches itself from the lander and unloads the payload. It could then remain on the surface to await more payloads or re-attach for unloading at a different site. Options for mobility are wheels, treads, walkers, and hoppers. A wheeled version of this concept is shown in Figure A.3.

An advantage of the detachable unloader is that it can precisely position the payloads. In addition, the payload could be placed out of range of the effects of the lander's rocket plume. This advantage reduces the amount of mass required for payload shielding. Since the unloader can be left on the lunar surface, the lander can deliver an increased amount of payload on return missions to the same site. The unloader could also be used as a construction tool.

The main disadvantage of the detachable unloader is that it requires a separate operating vehicle, with its own subsystems. These additional systems add to the complexity and mass of the design. The unloader also needs to be protected from the lunar environment when left on the surface for extended periods of time.

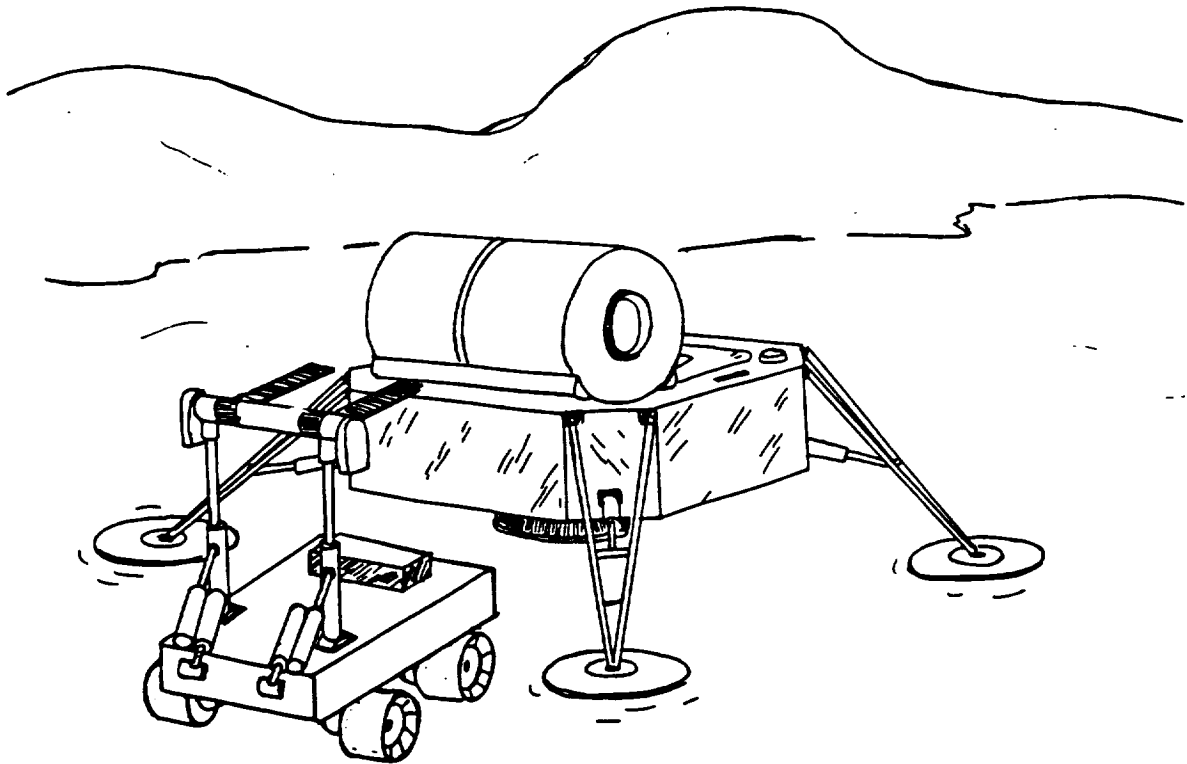


Figure A.3 The Wheeled Detachable Unloader

A.1.1.3 Mobile Lander

The Mobile Lander is a lander which can move on the lunar surface, place payloads, and move away before ascending. The same mobility options as for the Detachable Unloader can be used. Figure A.4 shows a mobile lander using moving legs.

Like the Detachable Unloader, the payload could be positioned more accurately and out of the way of the lander's rocket plume. The lander could also be used as a construction tool.

The disadvantage of this concept is the requirement for additional subsystems for mobility. These added subsystems would need to be re-lifted each trip, reducing the mass of payload it could carry.

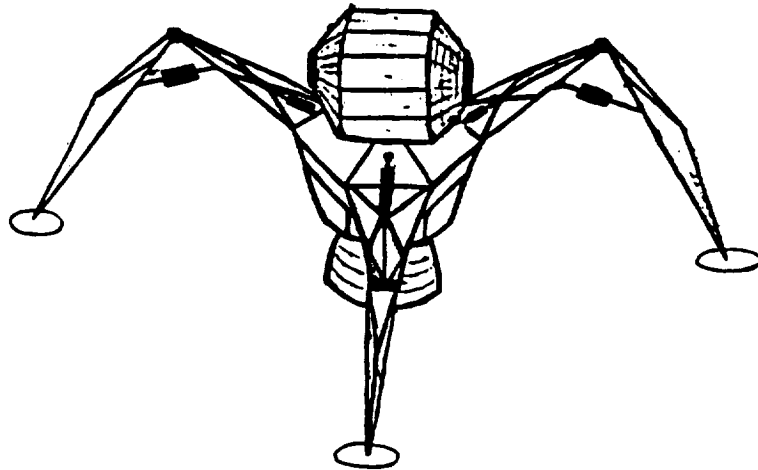


Figure A.4 The Mobile Lander with Moving Legs

A.1.1.4 Fixed Unloader

The Fixed Unloader concept consists of a traditional lander with a non-detachable unloading device. Figure A.5 shows a possible configuration of this concept.

One advantage of the Fixed Unloader is its simplistic design compared to other concepts. The Fixed Unloader also weighs less because it does not require the extra subsystems inherent in the other concepts.

The disadvantage of the Fixed Unloader is the need to carry the unloading device each trip. More importantly, the payload will be left close to the lander, requiring blast protection for the payload.

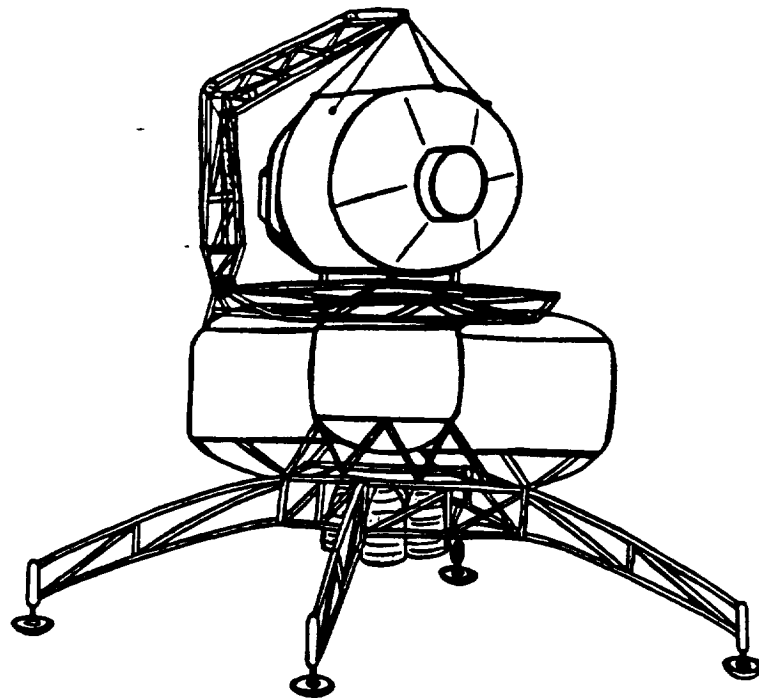


Figure A.5 The Fixed Unloader

A.1.2 Choosing Fixed Unloader Concept

In order to decide between the four preliminary concepts, the following criteria were used:

- mass
- complexity
- reliability
- power requirements

The Fixed Unloader concept was chosen because it provided the following: lower mass, fewer systems, less power, fewer moving parts, and simple operations. These features provide the Fixed Unloader with increased payload, increased reliability, and reduced cost.

A.2 Selection of Primary Design

Once the Fixed Unloader was chosen as the preliminary concept, five variations for unloading mechanisms were developed and evaluated. These variations are the following:

boom mechanism, manipulator arm, overhead unloader, bottom unloader, and ramp unloader.

A.2.1 Variations of the Fixed Unloader

The five main variations considered for the fixed unloader are:

- Boom Mechanism: similar to a boom used on the earth and driven by a motor and pulley system
- Manipulator Arm: a robotic arm comparable to the Shuttle's arm, but stronger
- Overhead Unloader: similar to unloading devices used on garbage trucks
- Bottom Unloader: lowers payload from the bottom of the lander

- Ramp: lowers payload down a ramp, which extends from the top of the lander

A.2.2 Choosing the Trolley Design

Using the same criteria of mass, complexity, reliability, and power requirements, the ramp and bottom unloader variations were chosen for further evaluation. The ramp variation was developed into the Trolley design and the bottom variation was developed into the Plunger and Donut designs. These designs are briefly described as follows:

- Trolley Unloader: a trolley system which runs along two rails from the top of the lander down to the bottom of the lander
- Plunger: a bottom unloading device in which a shaft raises and lowers the payload from the bottom of the lander
- Donut: a bottom unloading device in which the payload is lowered through a space in the center of the lander

In choosing the primary design, the following criteria were used in a decision matrix (Figure A.6):

- mass
- mechanical complexity
- engine placement
- refueling complexity
- docking complexity
- effects of lunar dust

Mass was weighted the highest because of its effect on cost and engine size. Mechanical complexity is related to the number of moving parts. Engine placement refers to how the placement of engines could affect the stability of the lander. Refueling complexity refers to the orientation and position of

the lander's fuel tanks relative to the OTV's fuel tanks. Docking complexity deals with the lander's ability to easily dock and transfer payload and fuel from the OTV. The effects of lunar dust refers to the resistance of the lander to the abrasiveness of lunar dust.

After evaluation of the design matrix, the Trolley unloader design was chosen. The Trolley design provides these favorable characteristics:

- engine out stability
- simple unloading operations
- top-docking with payload

These characteristics allow the Trolley system to fulfill the overall project requirements most effectively.

	Mass	Mechanical Complexity	Engine Placement	Refueling Complexity	Docking Complexity	Effect of Lunar Dust	TOTAL
WEIGHT	40	25	10	5	15	5	100
Donut	80	75	50	5	15	10	235
Plunger	80	50	50	25	60	10	275
Trolley	80	25	10	15	30	15	170

Figure A.6 The Primary Decision Matrix. Note: 1 is best and 5 is worst

Appendix B: Descent/Ascent Trajectory Models

Separate TK Solver models were developed for the descent and ascent trajectories. These models used the following assumptions:

- two-body restricted problem
- spherical moon
- instantaneous ΔV 's
- flat planet model for initial ascent and final descent.

Each of the models is separated into two phases: elliptical transfer orbits to and from the lunar surface and landing/takeoff trajectories. With the exception of a modified liftoff to clear the payload, the descent and ascent trajectories are identical. Each trajectory requires three ΔV 's, two for the beginning and end of the transfer ellipse and one for either takeoff or landing.

Using engine specifications and orbital and pitch-over altitudes, the models iteratively solve for transfer times, ΔV 's, burn times, and fuel required for each phase. These output parameters are optimized by varying the total fuel mass. The models are run using the following methodology:

1. The lander's dry mass is used in the ascent model to determine the amount of fuel required for ascent
2. The lander's dry mass, the payload mass, and 1.1 times the ascent fuel mass are added to determine the total wet mass of the lander before descent.
3. The wet mass of the lander, from step 2, is used in the descent model to determine the amount of fuel for descent.
4. The total amount of fuel required for one mission cycle is 1.1 times the sum of the masses from steps 1 and 3.

note: fuel masses include a factor of 1.1 to include fuel used during hover maneuvers and to compensate for boil off

VARIABLE SHEET					
St	Input	Name	Output	Unit	Comment
					Descent Model
<<< Constants >>>					
	6.627E-11	D		m ³ /kg*s	Universal Gravitational Constant
	5.9742E24	Mearth		kg	Mass of the Earth
		Mmoon	7.3483E22	kg	Mass of the Moon
	1738000	Rmoon		m	Radius of the Moon
		MuL	4.8697E12	m ³ /s	Gravitational Parameter of the Moon
		Gmoon	1.6121383	m/s ²	Surface Gravitational Accel. - Moon
	9.81	Ge		m/s ²	Surface Gravitational Accel. - Earth
	450	Isp		s	
<<< Orbit 1 ::: Circular Orbit >>>					
	200000	H1		m	Altitude of the Orbit
		R1	1938000	m	Orbital Radius
		V1	1695.1634	m/s	Orbital Velocity (circular)
<<< Propulsion 1 >>>					
L	560	M1	47594.417	kg	Total Lander Mass
		Mb1		kg	Mass of Fuel Burned
		M2	47594.417	kg	Total Lander Mass Remaining
		delV1	46.32694	m/s	Delta-V Provided
<<< Orbit 2 ::: Elliptical Orbit >>>					
		V2a	1509.6373	m/s	Apogee Velocity
		R2a	1938000	m	Apogee Radius
	250	H		m	Transfer Altitude
		R2	1738250	m	Transfer Points
		a1	1832456.7	m	Semi-Major Axis
		e2	.05758546		Eccentricity
		p2	1826380	m	Semi-Latus Rectum
		E	.06767744	rad	Mean Anomaly
L		V2	1716.2531	m	Transfer Velocity
		Ba2	.02400145	rad	Flight Path Angle at Transfer Point
		P12	7062.8542	s	Period
<<< Propulsion 2 >>>					
		Mb2	15262.826	kg	Mass of Fuel Burned
		M3	32133.598	kg	Total Lander Mass Remaining
		delV2	1715.672	m/s	Delta-V Provided
<<< Orbit 3 ::: Flat Moon Ballistic >>>					
L		V3x		m/s	X Component of Velocity
L		V3y	44.620014	m/s	Y Component of Velocity
L		t	60.482916	s	Freefall Time
		IV3y	-52.88681	m/s	Y Component of Velocity at Impact
L		IV3		m/s	Velocity at Impact
<<< Propulsion 3 ::: Braking >>>					
		Mb3	564.5981	kg	Mass of Fuel Burned
	31569	M4		kg	Total Lander Mass Remaining
		delV3	52.886811	m/s	Delta-V Provided
	158400	Th		N	Average [Constant] Thrust
		Mdot3	35.861753	kg/s	Average Mass Flow
L		Tb3	15.734564	s	Burn Time

Acc3 5.0175805 m/s^2

Maximum Acceleration

<< Totals >>>

L Mbt 16077.407

Propellant Mass Required

L delVT 1014.8848

Total Delta-V required

RULE SHEET

S Rule

"Lunar Deorbit and Descent

"Set Constants

* Mmoon/Mearth = 0.0123
* Gmoon = MuL/(Rmoon)^2
* MuL = G * Mmoon

"Orbit 1 :: Circular Orbit

* H1 = R1 - Rmoon
* V1 = sqrt(MuL/R1)

"Propulsion 1 :: Change Orbit to Ellipse

* M1 = Mb1 + M2
* delV1 = Ge*Isp*ln(M1/M2)
* V2a = V1 + delV1
* R2a = R1

"Orbit 2 :: Elliptical Transfer Orbit

* H2 = R2 - Rmoon
* .5*(V2a)^2 - MuL/R2a = - MuL/(2*a2)
* e2 = R2a/R1 - 1
* p2 = a2 * (1 - e2^2)
* cos(E) = (1 - R2/a2)/e2
* V2 = sqrt(-MuL * (2/R2 - 1/a2))
* tan(Ge2) = (e2 * sin(E)) / sqrt(1 - e2^2)
* Pt2 = 2*pi / sqrt(MuL/a2^3)

"Propulsion 2

* M2 = Mb2 + M3
* delV2 = Ge*Isp*ln(M2/M3)
* delV2 = V2 * cos(Ge2)
* V3y = V2 * sin(Gm2)

"Orbit 3 :: Final Descent

* -.5*Gmoon * t^2 + V3y*t + H2 = 0
* - Gmoon * t = V3y = IV3y
* IV3 = sqrt(IV3y^2 + V3y^2)

"Propulsion 3

* M3 = Mb3 + Mf
* delV3 = abs(IV3y)
* delV3 = Ge*Isp*ln(M3/Mf) - Gmoon*Tb3
* Mdot3 = Th/(Isp*Ge)
* Mb3 = Mdot3 * Tb3
* Acc3 = Th/Mf

"Totals

* MbT = Mb1 + Mb2 + Mb3
* delVT = delV1 + delV2 + delV3

ORIGINAL PAGE IS
OF POOR QUALITY

VARIABLE SHEET					
St	Input	Name	Output	Unit	Comment
					Ascent Model
					<<< Constants >>>
	6.627E-11	G			
	5.9742E24	Mearth			
		Mmoon	7.3483E22		
		MuL	4.8697E12		
	1738000	Rmoon			
	9.81	Ga			
		Gmoon	1.6121393		
	450	Isp			
					<<< Propulsion 1 >>>
		M1	16034.47		Mass at Blastoff
		Mb1	113.87624		Mass burned during Blastoff
		MR	15920.594		Mass Remaining after Blastoff
		deltaV1	17.956271		delta V from Blastoff maneuver
		Mdot	13.591572		Average Mass Flow
	60000	Th			Average (Constant) Thrust
L		Tbt	2.7784444		Burn time
		Acc1	3.7415384		Average (Constant) Acceleration
					<<< Orbit 1 >>>
		V1	17.956271		Initial Velocity
L		t1	11.13817		Time to apogee
	100	H1			Apogee altitude
					<<< Orbit 2 >>>
		RLn	100		Perigee altitude
		R3p	1738100		Perigee radius
	200000	ROa			Apogee altitude
		ROr	1938000		Apogee radius
		e	.05437828		Eccentricity
		a	1638050		semi-major axis
		V1p	1718.7463		Perigee Velocity
L		V2a	1541.4616		Apogee Velocity
		P-2	7095.2047		Period
					<<< Propulsion 2 >>>
		deltaV2	1718.7463		delta V
		Mb2	5134.3416		Mass burned
		MR	10786.252		Mass remaining
					<<< Orbit 3 >>>
		H3	200000		Orbital Altitude
		RO	1938000		Orbital Radius
		V3	1585.1634		Orbital Velocity
					<<< Propulsion 3 >>>
		Mb3	106.25244		Mass burned
	10680	M4			Mass left
		deltaV3	43.701639		delta V
					<<< Totals >>>
		Mprop	5754.4703		Total fuel required

LEV 1780.4047

Total delta V

ORIGINAL PAGE IS
OF POOR QUALITY

B6

RULE SHEET

5 Rule

"Lunar Ascent

"Set Constants

* Mmoon/Mearth = 0.0123
* MuL = G*Mmoon
* Gmoon = MuL/(Rmoon)^2

" Propulsion 1

* M1 = Mb1 +M2
* delV1 = Ge*Isp*ln(M1/M2) - Gmoon*Tb1
* Mdot1 = Th/(Isp*Ge)
* Mb1 = Mdot1 * Tb1
* Acc1 = Th/M1

" Orbit 1 :: Blastoff

* V1 = delV1
* - Gmoon * t + V1 = 0
* -0.5 * Gmoon * t^2 + V1 * t = H1

"Orbit 2 :: Ellipse

* R1 = R2p
* H2p = R2p - Rmoon
* R2a = R2p + Rmoon
* e = (R2a - R2p)/(R2a + R2p)
* a = (R2a + R2p)/2
* V2p = sqrt(MuL*(2/R2p - 1/a))
* V2a = sqrt(MuL*(2/R2a - 1/a))
* Ft2 = 2*apc()/sqrt(MuL/a^3)

"Propulsion 2

* delV2 = V2p
* M2 = Mb2 +M3
* delV3 = Ge*Isp*ln(M2/M3)

"Orbit 3

* R3 = RTa
* H3 = R3 - Rmoon
* V3 = sqrt (MuL/R3)

"Propulsion 3

* M3 = Mb3 +M4
* delV3 = V3 - V2a
* delV3 = Ge*Isp*ln(M3/M4)

"Totals

* Mprop =M1-M4
* DelV = delV1+delV2+delV3

ORIGINAL PAGE IS
OF POOR QUALITY

Appendix C: Rocket Exhaust Plume Effects

Due to its proximity to the lander, the effect of the rocket exhaust plume on the payload during take-off is a critical issue that must be addressed if this design is to succeed. The blast of the rocket could potentially knock the payload over, roll it away, or damage the payload with high velocity particles and high temperatures. Therefore, for this design to be feasible, the payload must be able to survive the take-off blast. Based on the analysis which follows, the payload will be able to survive the exhaust plume environment, provided adequate blast protection and deflection systems are used.

NASA has performed several tests to develop analytical methods for determining engine exhaust and surface interactions [C1:84-88 and 127-131]. Most of these tests have not produced analytical solutions, but rather, have mainly generated trends. Further testing is required if the effects of the rocket plume are to be better understood. The problem is very complex, but if future travel and exploration is to be made using rockets, its full effect in a space environment must be analyzed.

Since there are no current analytical methods for determining the effects of the rocket exhaust plume, the forces acting on the payload can only be approximated. Two computer simulations of the exhaust plume have been discovered, but B&T Engineering has been unable to acquire either of these. To further understand the gas flow leaving the exhaust, at least one of these computer programs should be run to determine the gas properties, and thus give a better prediction of the forces acting on the payload. One method employs a momentum integral technique, which predicts the thermodynamic properties of the decaying rocket exhaust

plume [C2:2385]. The other simulation uses a Direct Simulation Monte Carlo (DSMC) method to predict the mass flux density in the plume of a bipropellant engine [C3:1857]. Either of these models might better estimate the pressures, velocities, temperatures, and mass flow rates acting on the payload than the analysis given in this report.

C.1 Analysis

In order to estimate the forces on the payload during take-off, an analysis of the fluid dynamics was conducted. This section lists some assumptions, describes the methods and reasoning, and discusses two of the models which were used.

C.1.1 Assumptions

To conduct any analysis on a process as complicated as gas and soil dynamics in a vacuum, several major assumptions must be made to simplify the problem. The assumptions in this report are made so that the estimated effects of the blast are as large as possible without being unrealistic. Some were made based on discussions with several professors and others were made based on information acquired through research, and on judgment. The following is a list of the major assumptions:

1. The particles leaving the exhaust plume act as a perfect gas;
2. All gas expansion is isentropic with no heat or friction loss;
3. The ambient pressure on the moon is zero;
4. The expanding gas crosses a shock formed in the expanding fluid after it leaves the engine cone;
5. The gas expands radially from the lander after crossing the shock;

6. The equivalent thrust of the gas after it crosses the shock is distributed equally as the gas expands;
7. The force on the payload is caused by the gas particles and the pressure over its cross-section in the gas flow;
8. The lunar soil is fixed and only acts to turn the flow.

Any other assumptions made are stated as they arise in the rocket plume model development.

C.1.2 Rocket Plume Model Development

The force exerted on the payload by the rocket plume consists of two parts: the macroscopic gas motion and the microscopic gas motion known as pressure. The force is related to these components by the equation [C4:356]

$$F = m u_p + (P_p - P_a) A_p$$

where F is the force on the payload, m is the mass flow rate hitting the payload, u_p is the velocity of the particles hitting the payload, P_p is the pressure of the gas when it hits the payload, P_a is the ambient pressure of the atmosphere, and A_p is the cross-sectional area of the payload which is hit by the gas. The ambient pressure on the moon is zero, so it drops from the equation. If these values can be estimated, the force can be approximated.

To compute the mass flow rate that would strike the payload, a percentage of the total mass flow rate based on the ratio of the payload area to the expansion area is used. The total mass flow rate for the rocket plume can be computed using the equation [C4:356]

$$m_{\text{tot}} = \frac{A^* P_0}{\sqrt{RT_0}} \sqrt{\gamma \left(\frac{2}{\gamma+1} \right)^{\frac{\gamma+1}{\gamma-1}}}$$

where m_{tot} is the total mass flow rate through the rocket engines, A^* is the nozzle throat area of the rocket engines, P_0 is the stagnation pressure of the gas, R is the gas constant of the gas, T_0 is the stagnation temperature of the gas, and γ is the ratio of specific heats of the gas.

Then the mass flow rate across the payload can be computed using

$$m = m_{\text{tot}} \frac{A_p}{A_r}$$

where A_r is the surface area of the expanding gas.

Estimation of the gas velocity and the pressure is a little more difficult. This requires analyzing the dynamics of each phase of the expansion: from the rocket nozzle throat, through the rocket nozzle, out the exit plane, across a shock, and expanding out towards the payload, as shown in Figure C.1. From the nozzle throat to the exit plane, the gas accelerates to a specific Mach number based on the ratio of the exit plane area to the throat area, as shown in the equation [C4:49]

$$M_e = \frac{A^*}{A_e} \left[\frac{2}{\gamma+1} \left(1 + \frac{\gamma-1}{2} M_e^2 \right) \right]^{\frac{\gamma+1}{2(\gamma-1)}}$$

where M_e is the Mach number of the gas at the exit plane of the rocket nozzle, and A_e is the area of the exit plane. To solve for the Mach number an iterative approach must be used.

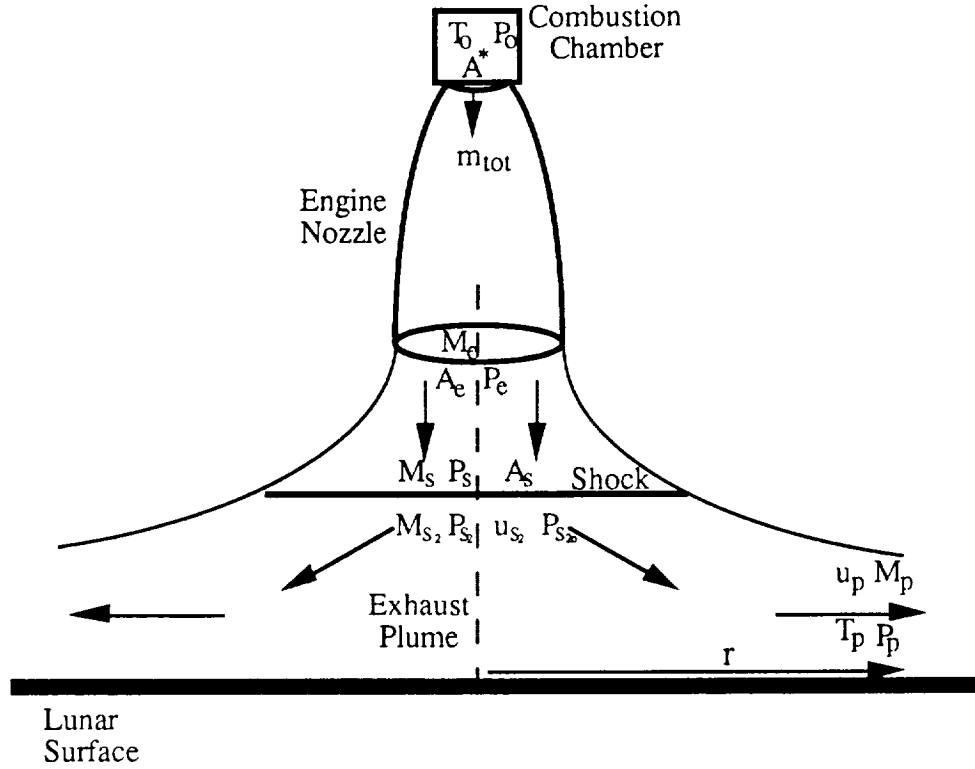


Figure B.1 Rocket Exhaust Plume Flow Model

Once the Mach number at the exit is known, the Mach number just before the shock can be estimated by the approximation [C5]

$$M_s = 1.5M_e$$

where M_s is the Mach number of the gas just before the shock. With the Mach number before the shock calculated, the pressure and expanded area before the shock can be computed using [C4:47-49]

$$P_s = \frac{P_0}{\left(1 + \frac{\gamma-1}{2} M_s^2\right)^{\frac{\gamma}{\gamma-1}}}$$

and

$$A_s = \frac{A^*}{M_s} \left[\frac{2}{\gamma+1} \left(1 + \frac{\gamma-1}{2} M_s^2 \right) \right]^{\frac{\gamma+1}{2(\gamma-1)}}$$

where P_s is the pressure of the gas just before crossing the shock, and A_s is the cross-sectional area of the gas when it hits the shock.

The gas then passes through a shock and the new Mach number, pressure, stagnation pressure and velocity can be computed using [C4:47 and 58]

$$M_{s_2} = \sqrt{\frac{M_s^2 + \frac{2}{\gamma-1}}{\frac{2\gamma}{\gamma-1}M_s^2 - 1}}$$

$$P_{s_2} = P_s \left[\frac{2\gamma}{\gamma+1}M_s^2 - \frac{\gamma-1}{\gamma+1} \right]$$

$$P_{s_{2o}} = P_o \left[\frac{\left(\frac{\gamma+1}{2}M_s^2 \right)}{\left(1 + \frac{\gamma-1}{2}M_s^2 \right)} \right]^{\frac{\gamma}{\gamma-1}} \left(\frac{2\gamma}{\gamma+1}M_s^2 - \frac{\gamma-1}{\gamma+1} \right)^{\frac{-1}{\gamma-1}}$$

and

$$u_{s_2} = M_{s_2} \sqrt{\frac{\gamma R T_o}{1 + \frac{\gamma-1}{2}M_{s_2}^2}}$$

where M_{s2} , P_{s2} , P_{s2o} , and u_{s2} are, respectively, the Mach number of the gas, the pressure of the gas, the stagnation pressure of the gas, and the velocity of the gas, all after crossing the shock.

After the shock, a new equivalent thrust is generated based on the new velocity, pressure, and area using an equation similar to the force equation. From this point in the expansion on, this force is used as the thrust at a given distance from the lander. Also, a new equivalent nozzle throat area is produced, since the stagnation pressure and Mach number have changed. This can be calculated using [C4:356]

$$A_2^* = \frac{m_{tot} \sqrt{RT_o}}{P_{s_{2o}} \sqrt{\gamma \left(\frac{2}{\gamma+1} \right)^{\frac{\gamma+1}{\gamma-1}}}}$$

where A_2^* is the equivalent nozzle throat area.

Then, the Mach number, the pressure, the temperature, and the velocity at the payload location can be computed using [C4:47-49 and 356]

$$M_p = \frac{A_2^*}{A_r} \left[\frac{2}{\gamma+1} \left(1 + \frac{\gamma-1}{2} M_p^2 \right) \right]^{\frac{\gamma+1}{2(\gamma-1)}}$$

$$P_p = \frac{\tau_2}{A_r} - \frac{A_2^* P_{s_{2o}}}{A_r} \sqrt{\frac{2\gamma^2}{\gamma-1} \left(\frac{2}{\gamma+1} \right)^{\frac{\gamma+1}{\gamma-1}} \left[1 - \left(\frac{P_p}{P_{s_{2o}}} \right)^{\frac{\gamma-1}{\gamma}} \right]}$$

$$T_p = \frac{T_o}{1 + \frac{\gamma-1}{2} M_p^2}$$

and

$$u_p = M_p \sqrt{\frac{\gamma R T_o}{1 + \frac{\gamma-1}{2} M_p^2}}$$

where M_p , P_p , T_p , and u_p are , respectively, the Mach number, pressure, temperature, and velocity of the gas at the payload. These equations must be solved iteratively.

Once the mass flow rate, the velocity of the gas, and the pressure of the gas are known, the force on the payload can be estimated using the force equation. The expansion area and payload area are discussed in the section about rocket plume models.

C.1.3 Rocket Plume Expansion Models

Two rocket plume models are considered: a radially expanding disk and a radially expanding hemisphere. The expanding disk model simply assumes that after the gas crosses the shock it expands radially in only two dimensions, while the expanding hemisphere expands in three

dimensions. Both models are identical except for the equivalent exit area at the payload's distance from the lander.

C.1.3.1 Disk Model

The expanding disk model is shown in Figure C.2. Here the gas is assumed to expand radially in a disk, without growing in height. This model is based on a study of a rocket plume hitting a flat plate. In that report, which was conducted with an atmosphere, after passing through the shock the plume expanded similar to a disk. In this model the expansion area is given by

$$A_r = 2\pi rh$$

where r is the radial distance from the center-line of the engines and h is the height of the expanding cylinder.

C.1.3.2 Hemisphere Model

The expanding hemisphere model is shown in Figure C.3. Here the gas is assumed to expand radially in all directions. This model assumes that since there is no atmosphere on the moon, the gas will try to expand in all directions to fill the vacuum. In order to better estimate the expansion around the lander, the cross-sectional area of the lander is removed from the expanded area. In this model the expansion area is given by

$$A_r = 2\pi r^2 - A_L$$

where A_L is the cross-sectional area of the lander.

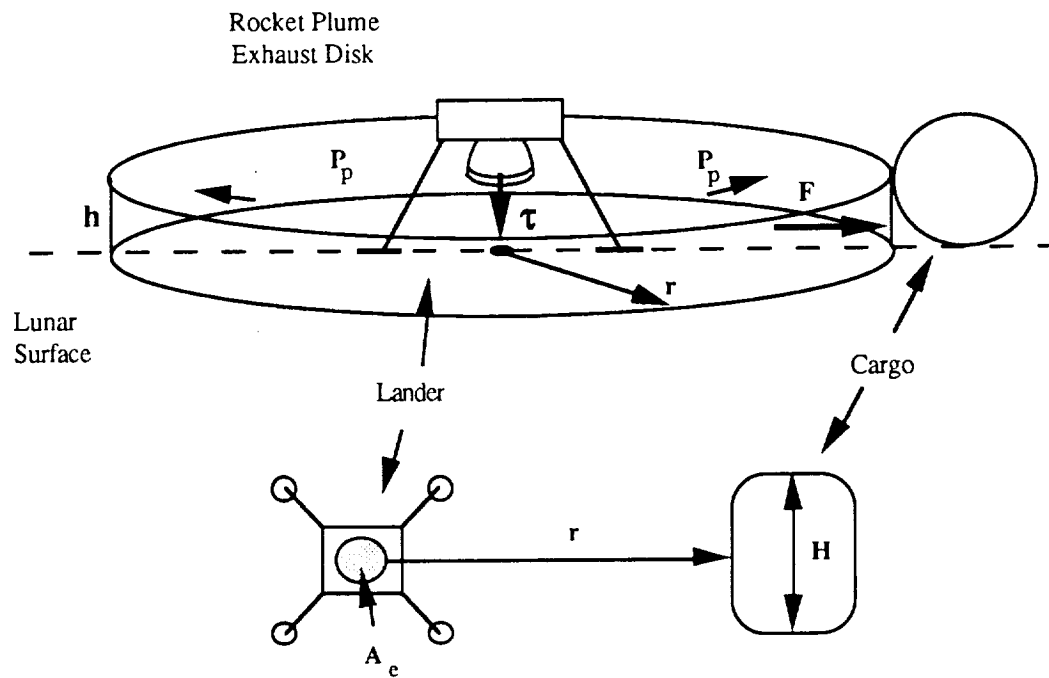


Figure B.2 The Expanding Disk Model

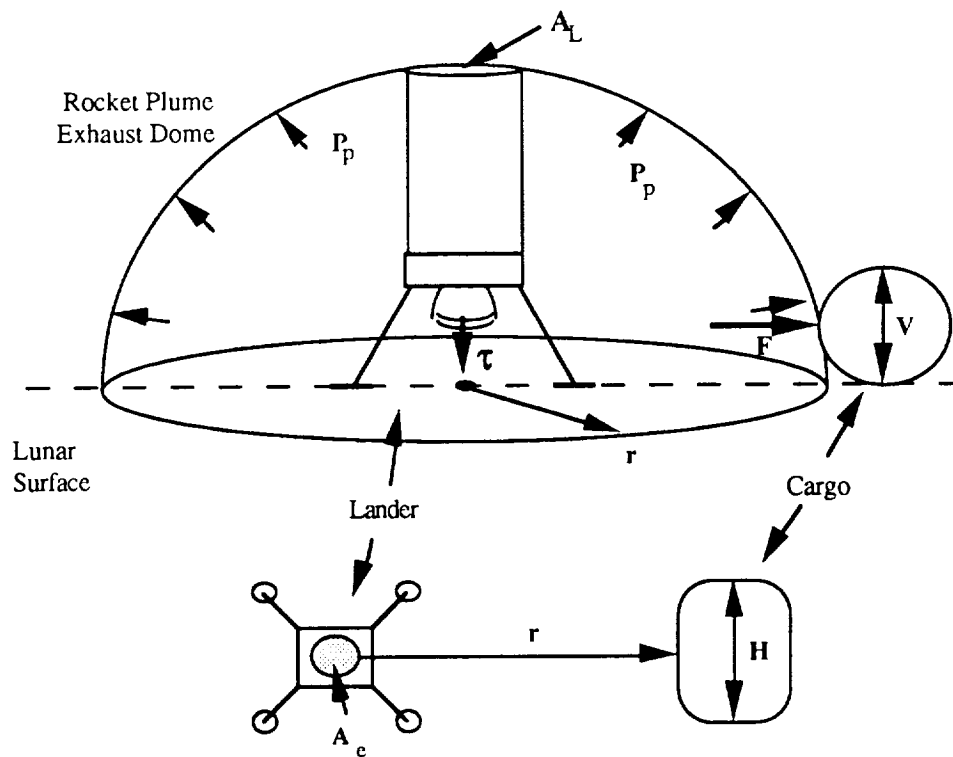


Figure B.3 The Expanding Hemisphere Model

C.2 Results

Using the thrust and engine data for the lander, the estimated forces on the payload were computed for both models using the TK Solver models given in Tables C.1, C.2, and C.3, and the results are shown in Figure C.4 as functions of radial distance from the engines' center line. This indicates that at the payload distance of 9 meters, the force acting on it will be about 2000 newtons and the temperature will be 3500 degrees Kelvin.

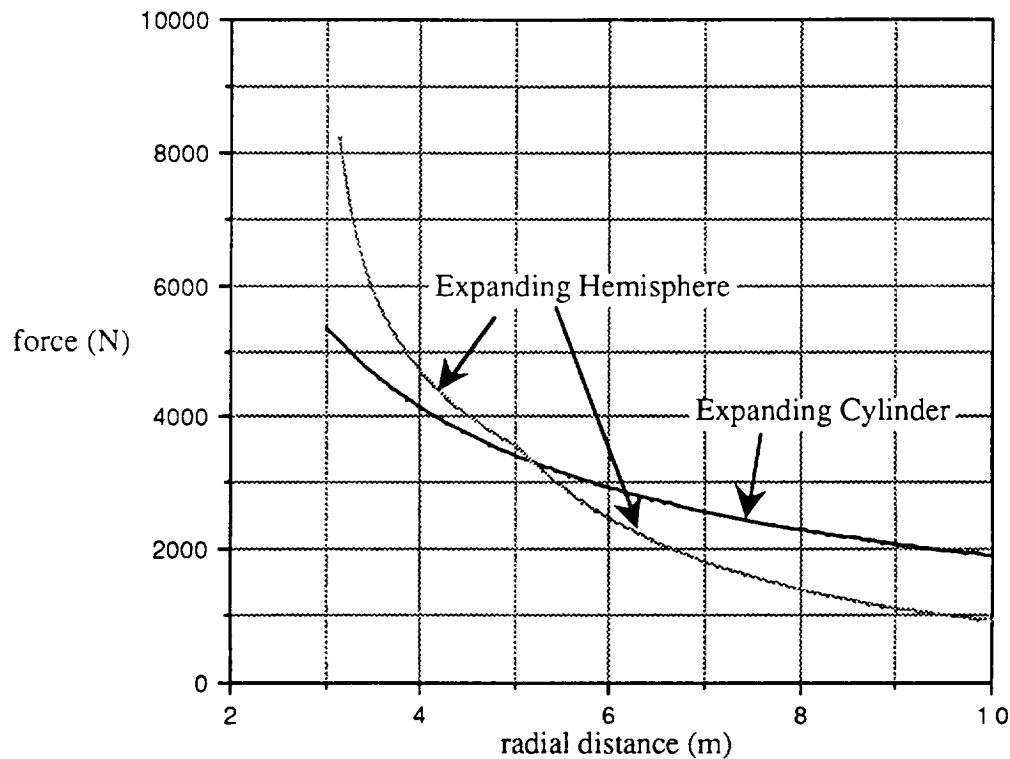


Figure B.4 Force on Payload versus Radial Distance from Engine Centerline for a Thrust of 60000 N

C.3 Conclusions

Since our rocket plume models do not include parameters for heat loss and energy conversion, the forces calculated here should be larger than the real forces, assuming the gas is expanding isentropically. During an actual take-off, the gas from the exhaust transfers some of its energy to

the lunar soil in the form of heat and kinetic energy. The lunar dust will take some the energy from the blast by removing kinetic energy when the fluid is turned ninety degrees at lunar impact, causing the gas to slow down even faster as it expands. Some of the initial impact of the fluid with the lunar surface will be directly converted to heat, thus slightly raising the temperature of the surface, again removing energy from the fluid. Also, since there is no ambient pressure the fluid will tend to disperse itself as much as possible, causing the gas travelling radially from the engines to expand upward and much of the thermal energy to disperse as radiation.

Based on these results, the payload should be in no major danger from the exhaust plume, as long as there is adequate protection from stray high speed particles and high temperatures. This protection will only be required for about 8 seconds, which is the time required for the lander to take-off and attain an altitude of about 100 meters where the exhaust no longer influences the payload. Selection of the protective material should be made based on these needs and its weight. Some type of bracing device or blast deflector may be required to prevent the payload from being pushed or rolled. This device would only be required to counter-balance the force and moment applied to the payload by the expanding gas.

C.4 References

- C1. Jet Propulsion Laboratory and California Institute of Technology, Flight Projects, Space Programs Summary 37-47 Vol.1, for the period July 1 to August 31, 1967: Pasadena, California, September 1967.
- C2. Nourse, Roswell W., "A Numerical Routine for Defining Rocket Exhaust Characteristics and Impingement Effects, Technical Report, for period ending Jun. 1988", abstract from Scientific and Technical Aerospace Reports. NASA: Vol.27 No.17, 8 September 1989.
- C3. Doo, Yi C. and Nelson, Duane A., "Direct Monte Carlo Simulation of Small Bipropellant Engine Plumes, Final Report, Mar. 1985 - May 1986", abstract from Scientific and Technical Aerospace Reports. NASA: Vol.25 No.14, 23 July 1987.
- C4. Hill, Philip G. and Peterson, Carl R., Mechanics and Thermodynamics of Propulsion. Reading, Massachusetts: Addison-Wesley Publishing Co., 1970.
- C5. Westkaemper, Dr. John C., Consultations . University of Texas at Austin, 1990

Table C.1 Variable Sheet for both Expansion Models

St	Input	Name	Output	Unit	Comment
		R	519.6625	$\text{m}^2/\text{s}^2/\text{K}$	gas constant
	8314.6	Rbar		$\text{kg}\cdot\text{m}^2/\text{s}^2$	universal gas constant
	16	Mbar		kg/kmole	molecular weight of gas
		Bgam	.34885901		
	1.22	gam			ratio of specific heats
		Cgam	.11		
		Dgam	.18032787		
		mdot	18.198146	kg/s	mass flow rate
	.0141	Astar		m^2	nozzle throat area
	889357.98	Po		N/m^2	stagnation pressure
	3500	To		K	stagnation temperature
	20000	t		N	thrust
	57	n			ratio of throat to exit areas
		As	5.6902924	m^2	area at shock
		Ms	6.2049553		Mach number before shock
		Ms2	.33423783		Mach number after shock
		Ps2o	4141.8411	N/m^2	stagnation press. after shock
L		Ar	18.849556	m^2	area at cargo location
L	3	r		m	radial distance from exhaust
		x		m	height of cylinder
L		Ap	15	m^2	cargo cross-sectional area
	5	h		m	cargo width
	5	v		m	cargo height
		Astar	2 9.0828792	m^2	equiv. throat area after shock
LG	657.88893	Pr		N/m^2	pressure at cargo
LG	2.1029176	Mr			Mach number at cargo
L		Tr	2354.605	K	temperature at cargo
L		Ur	2569.3419	m/s	velocity at cargo
L		Fr	47076.578	N	force on cargo
		Ps	91.681645	N/m^2	pressure before shock
		t2	31030.293	N	force after shock
		Us	494.85509	m/s	velocity after shock
		Ps2	3870.6003	N/m^2	pressure after shock
		Ae	.8037	m^2	exit area of nozzle
		vp	3	m	vert. cargo dimension in flow
	2509.6826	Pe		N/m^2	pressure at exit
	4.1366369	Me			Mach number at exit

Table C.2 Rule Sheet for Expanding Cylinder Model

S Rule

$$* R = R_{\text{bar}} / M_{\text{bar}}$$

$$* B_{\text{gam}} = (2 / (\text{gam} + 1))^{\text{gam} / (\text{gam} - 1)}$$

$$* C_{\text{gam}} = (\text{gam} - 1) / 2$$

$$* D_{\text{gam}} = (\text{gam} - 1) / \text{gam}$$

$$* A_e = n * A_{\text{star}}$$

$$* P_o = \sqrt{(P_e * (1 + C_{\text{gam}} * M_e^2)^{1/D_{\text{gam}}})^2}$$

$$* P_e = \sqrt{(t / A_e - A_{\text{star}} * P_o / A_e * \sqrt{\text{gam}^2 / C_{\text{gam}} * B_{\text{gam}} * (1 - (P_e / P_o)^{D_{\text{gam}}})})^2}$$

$$* \text{mdot} = 3 * A_{\text{star}} * P_o * \sqrt{\text{gam} * B_{\text{gam}} / R / T_o}$$

$$* M_s = 1.5 * M_e$$

$$* A_s = A_{\text{star}} / M_s * (2 / (\text{gam} + 1) * (1 + C_{\text{gam}} * M_s^2))^{\text{gam} / (2 * (\text{gam} - 1))}$$

$$* P_s = P_o / (1 + C_{\text{gam}} * M_s^2)^{1/D_{\text{gam}}}$$

$$* M_{s2} = \sqrt{(M_s^2 + 1 / C_{\text{gam}}) / (\text{gam} / C_{\text{gam}} * M_s^2 - 1)}$$

$$* P_{s2o} = P_o * (((\text{gam} + 1) / 2 * M_s^2) / (1 + C_{\text{gam}} * M_s^2))^{1/D_{\text{gam}}} / (2 * \text{gam} / (\text{gam} + 1) * M_s^2 - (\text{gam} - 1) / (\text{gam} + 1))^{1/(\text{gam} - 1)}$$

$$* P_{s2} = P_s * (2 * \text{gam} / (\text{gam} + 1) * M_s^2 - (\text{gam} - 1) / (\text{gam} + 1))$$

$$* U_s = M_{s2} * \sqrt{\text{gam} * R * T_o / (1 + C_{\text{gam}} * M_{s2}^2)}$$

$$* t_2 = \text{mdot} * U_s + P_{s2} * A_s$$

$$* A_r = 2 * \text{PI}() * r^2$$

$$* A_p = 10$$

$$* A_{\text{star}2} = \text{mdot} / P_{s2o} * \sqrt{R * T_o / \text{gam} / B_{\text{gam}}}$$

$$* M_r = A_{\text{star}2} / A_r * (2 / (\text{gam} + 1) * (1 + C_{\text{gam}} * M_r^2))^{\text{gam} / (2 * (\text{gam} - 2))}$$

$$* P_r = \sqrt{(t_2 / A_r - A_{\text{star}2} * P_{s2o} / A_r * \sqrt{\text{gam}^2 / C_{\text{gam}} * B_{\text{gam}} * (1 - (P_r / P_{s2o})^{D_{\text{gam}}})})^2}$$

$$* T_r = T_o / (1 + C_{\text{gam}} * M_r^2)$$

$$* U_r = M_r * \sqrt{\text{gam} * R * T_o / (1 + C_{\text{gam}} * M_r^2)}$$

$$* F_r = A_p / A_r * \text{mdot} * U_r + P_r * A_p$$

Table C.3 Rule Sheet for Expanding Hemisphere Model

S Rule

- * $R = R_{bar}/M_{bar}$
- * $B_{gam} = (2./(gam+1.))^{((gam+1.)/(gam-1.))}$
- * $C_{gam} = (gam-1.)/2.$
- * $D_{gam} = (gam-1.)/gam$
- * $A_e = n * A_{star}$
- * $Po = \sqrt{(Pe * (1 + C_{gam} * Me^2)^{(1/D_{gam}}))^2}$
- * $Pe = \sqrt{(t/A_e - A_{star} * Po / A_e * \sqrt{gam^2 / C_{gam} * B_{gam} * (1 - (Pe/Po)^{D_{gam}}))})^2}$
- * $\dot{m} = 3 * A_{star} * Po * \sqrt{gam * B_{gam} / R / To}$
- * $M_s = 1.5 * Me$
- * $A_s = A_{star} / M_s * (2./(gam+1) * (1 + C_{gam} * M_s^2))^{((gam+1)/(2*(gam-1)))}$
- * $Ps = Po / (1 + C_{gam} * M_s^2)^{(1/D_{gam})}$
- * $M_{s2} = \sqrt{(M_s^2 + 1./C_{gam}) / (gam / C_{gam} * M_s^2 - 1.)}$
- * $Ps2o = Po * (((gam+1.)/2. * M_s^2) / (1 + C_{gam} * M_s^2))^{(1./D_{gam})} / (2. * gam / (gam+1.) * M_s^2 - (gam-1)/(gam+1))^{(1/(gam-1))}$
- * $Ps2 = Ps * (2. * gam / (gam+1) * M_s^2 - (gam-1)/(gam+1))$
- * $U_s = M_{s2} * \sqrt{gam * R * To / (1 + C_{gam} * M_{s2}^2)}$
- * $t2 = \dot{m} * U_s + Ps2 * A_s$
- * $Ar = 2. * PI() * r^2 - b^2$
- * if $r < 5$ then $vp = r$ else $vp = 5$
- * $Ap = h * vp$
- * $A_{star2} = \dot{m} / Ps2o * \sqrt{R * To / gam / B_{gam}}$
- * $Mr = A_{star2} / Ar * (2./(gam+1) * (1 + C_{gam} * Mr^2))^{((gam+1)/(2*gam-2))}$
- * $Pr = \sqrt{(t2 / Ar - A_{star2} * Ps2o / Ar * \sqrt{gam^2 / C_{gam} * B_{gam} * (1 - (Pr/Ps2o)^{D_{gam}}))})^2}$
- * $Tr = To / (1 + C_{gam} * Mr^2)$
- * $Ur = Mr * \sqrt{gam * R * To / (1 + C_{gam} * Mr^2)}$
- * $Fr = Ap / Ar * \dot{m} * Ur + Pr * Ap$

Appendix D: Vehicle Illustration

The purpose of this appendix illustrates the lunar lander. All possible sides and surfaces of the vehicle are shown in Figures D.1 through D.4. These pictures are added to give a better understanding of the geometry and shape of the lander.

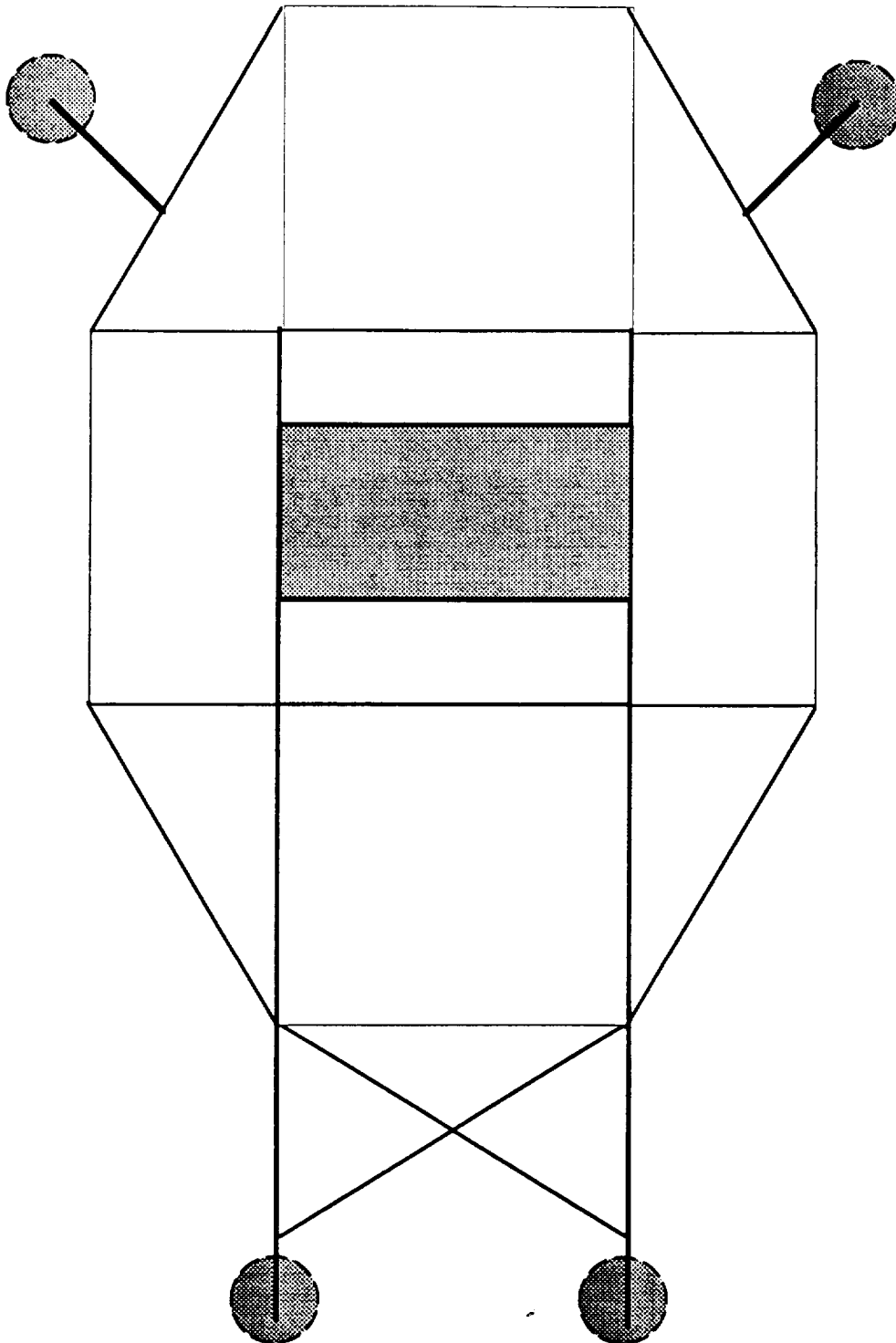


Figure D.1 Top View of Lander

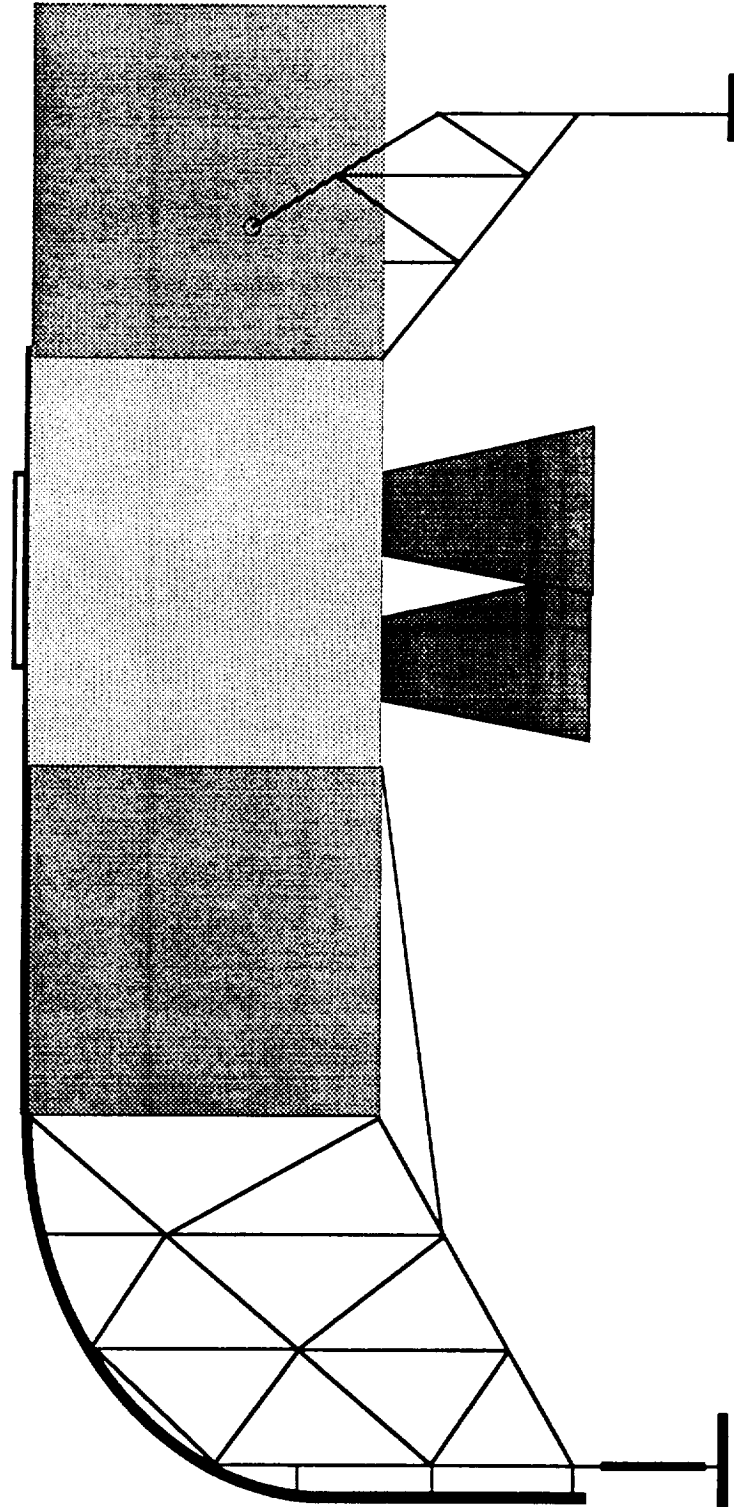


Figure D.2 Side View of Lander

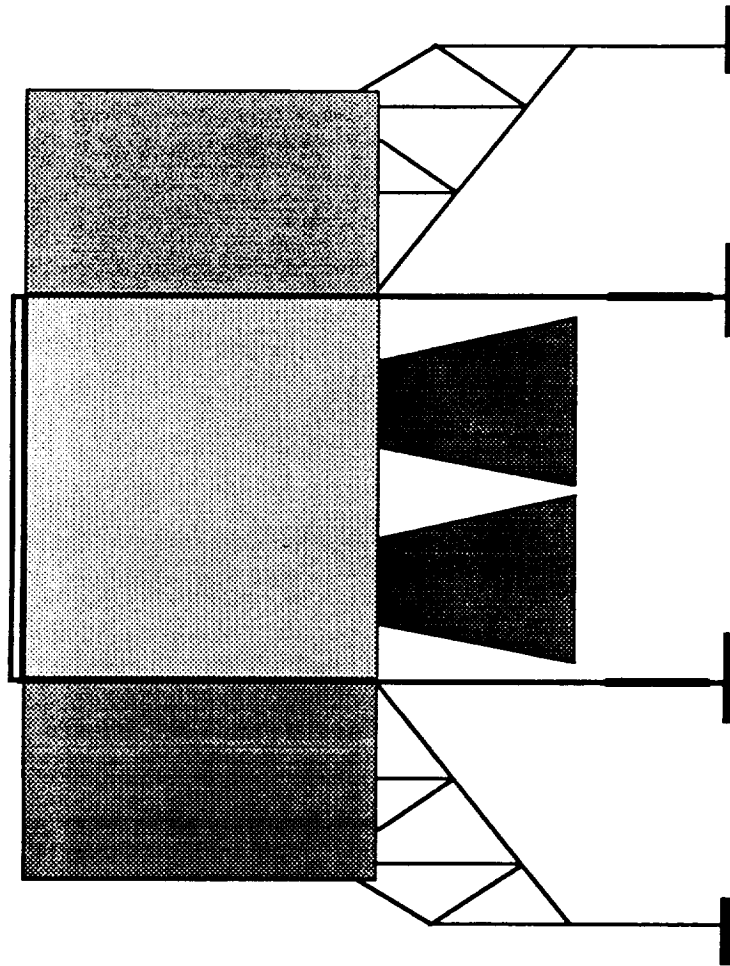


Figure D.3 Front View of Lander

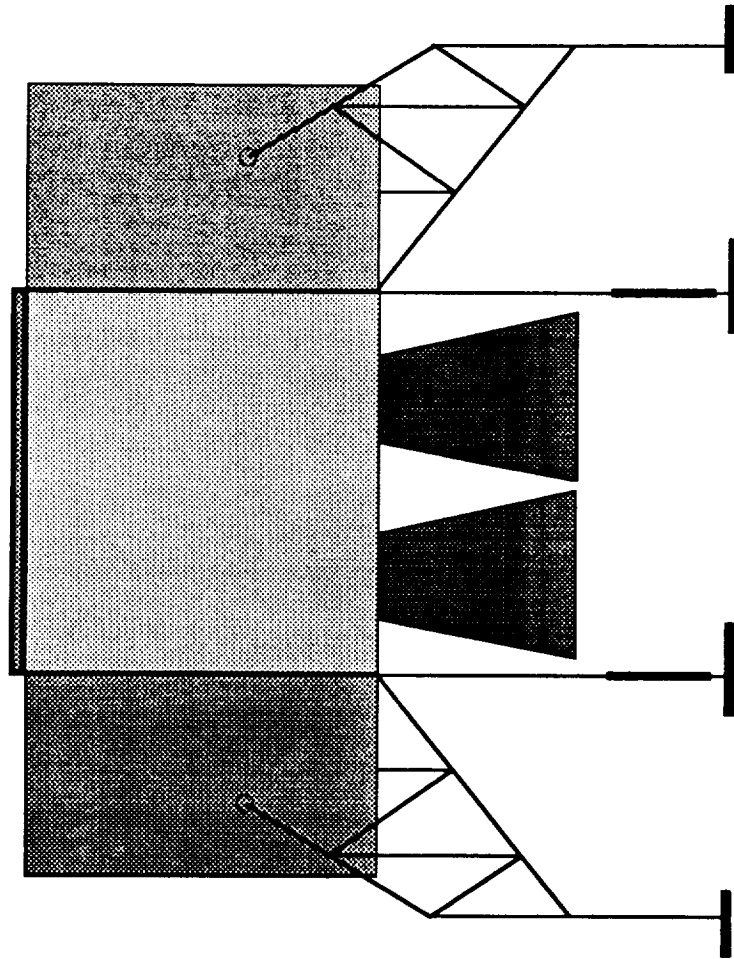


Figure D.4 Rear View of Lander

Appendix E: Propulsion

For many orbital and space missions, high specific impulse (Isp) propellant combinations are desirable. Since the nature of our mission is to transport 15000 kg to the surface of the moon for LLO, the propulsion system had to be very powerful. Therefore, nuclear and solar methods of propulsion were excluded. Chemical propulsion is the only method available that can provide the large thrust required for our mission. The choice of the main engines hinged on the engines fuel efficiency (Isp). Those that burn liquid hydrogen and liquid oxygen provide the highest thrust and Isp. Therefore, liquid hydrogen and oxygen were chosen as the propellant for the lander. The characteristics of a hydrogen oxygen mixture are shown below in Table E.1 [17].

Table E.1 Hydrogen and Oxygen Performance Characteristics

Mixture Ratio by Weight	3.5
by Volume	.21
Average Specific Gravity, (g/cc)	.26
Chamber Temperature, (°F)	5870
Specific Impulse, (sec)	450
Ratio of Specific Heats	1.22
Bulk Density, (gm/cm ³)	.43

The liquid hydrogen and oxygen must be stored as cryogenic liquids. Baffle storage tanks with insulation are proposed to control sloshing and boiloff. The volume of the tanks were determined from the ΔV requirements of the mission. The tanks were modeled spherically in order to obtain maximum capacity with losing structural integrity.

The next process in deriving the propulsion system was to determine the number of engines required on the lander. Studies conducted by Aerojet, Pratt & Whitney, and Rocketdyne determined that three engines are favorable and most efficient from an engine-out stand point. Therefore, calculations were performed to determine the maximum thrust required for the mission. This thrust level was found to be 54,629 lbs and occurred when performing a three 'g' landing (Appendix F). Therefore, engines that can provide 30,000 lbs of thrust are needed to satisfy the engine-out scenario. This requirement results in a thrust level of 60% for all three engines operating and 90% for two engines operating. The engine performance characteristics are shown below in Table E.2.

Table E.2 Engine Performance

Propellant	LO2/LH2
Engine Cycle	Closed Expander
Thrust, lbf (vac)	20,000
Spec. Impulse, (sec)	477
Gimbal, (deg)	6 - 10
Chamber pressure, psia	1900
Mixture ratio (O/F)	6/1
Expansion ratio	200/450
Exit diameter, (in)	45/68
Length, (in)	63/126
Weight, (lbm)	1000

With the six to ten degree gimbaling capability, the center of gravity range can be seen in Figure 7.1.

Appendix F: Sample Calculations for Thrust

$M_{\text{payload}} = 15000 \text{ kg}$

$M_{\text{structure}} = 30\% M_{\text{payload}}$

$M_{\text{fuel}} = 16000 \text{ kg}$

Descent (3 g's)

$$\begin{aligned} W &= mg = (50000 \text{ kg}) * (1.62 \text{ m/sec}^2) \\ &= 81000 \text{ N} \end{aligned}$$

$$\begin{aligned} \text{Thrust (T)} &= W * (3 \text{ g's}) \\ &= 243000 \text{ N} \\ &= 54629 \text{ lbf} \end{aligned}$$

where $1 \text{ lbf} = 4.4482 \text{ N}$

* Use three engines at 60% thrust level. With two engines on the thrust level will be 90%.

Appendix G: Battery Sizing TK Solver Model

This appendix contains the TK Solver model used to compute the size of sodium-sulfide (NaS) batteries and the depth of discharge during peak power usage.

VARIABLE SHEET					
St	Input	Name	Output	Unit	Comment
		msstruc	6.7627553		Mass of struc for solar cells
		areacel	7.7951668		Area of solar cells
		mscell	3.3407601		Mass of solar cells
		volbat	.02239055		battery volume (cubic meters)
		mbat	92.066406		battery mass
		pmadpss	.60741092		Mass of power man and distribution
		total	102.79733		total mass
		dia	7.5556076		% battery discharged/night
		engener	1.75		Engine energy consumption
.175		engtime			Engine Run Time
10		engnep			Engine power consumption
		misener	2.5935		Energy from OTV to parking orbit
6.175		misetime			Mission Time from OTV to parking orbit
		totalene	5.44795		Total mission energy (kWh)
.19355		motener			Motor energy req.
		balener	5.89225		energy required for batteries
.42		nompon			nominal power consumption
2.12		oritime			orbital period (hours)
12.5		batap			battery specific power, kg/kWh
.0039		batav			battery specific volume
		solarpc	1.0123515		power required from solar arrays
		nightpo	.91172314		recharge night power
		ptakpcw	.08062737		recharge mission power
.67		baleff			battery recharge efficiency
160		etime			between mission time (hours)
3.3		mscell			specific mass of solar cells
7.7		msarea			specific area of solar cells
6.7		msstruc			specific mass of cell struc
.6		mpand			specific mass of PMAO
1		mgener			Energy required for CMEs/mission

ORIGINAL PAGE IS
OF POOR QUALITY

RULE SHEET

```

S Rule
* engenergy=engtime*enginepow
* misenergy=disttime*nompow
* peakenergy=engenergy+misenenergy+motenergy+cmgenenergy
* batenergy=psakeenergy+orbtime*nompow/2
* mbat=batcap*batenergy/.5
* volbat=batcap*batenergy
* solarpow=capow+nightpow+peakpow
* nightpow=orbtime*.5*nompow/bateff
* dis=100*nompow*orbtime*.5/batenergy
* peakpow=batenergy*(1/bateff)/(btime/2)
* msceil=solarpow*msceil1
* areacell=solarpow*ssarea
* mestruc=solarpow*smestruc
* pmadmass=ampand*solarpow
* total=mestruc+msceil+mbat+pmadmass

```

ORIGINAL PAGE IS
OF POOR QUALITY